Applied Catalysis B: Environment and Energy 345 (2024) 123707

Contents lists available at ScienceDirect

Applied Catalysis B: Environment and Energy

journal homepage: www.elsevier.com/locate/apcatb

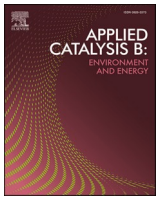

Unbiased photoelectrochemical carbon dioxide reduction shaping the future of solar fuels

Haijiao Lu, Lianzhou Wang *

Nanomaterials Centre, School of Chemical Engineering, and Australian Institute for Bioengineering and Nanotechnology, The University of Queensland, St Lucia, QLD 4072, Australia

ARTICLE INFO

Keywords:
Photoelectrochemical
Carbon dioxide reduction
Solar fuels
Tandem cell
Photovoltaic

ABSTRACT

As atmospheric carbon dioxide (CO_2) levels surge due to human activities, addressing this global crisis is paramount. This article delves into the realm of photoelectrochemical (PEC) CO_2 reduction, a promising solution that combines solar energy conversion and electrochemical processes to transform CO_2 into clean energy fuels. The primary focus of this article lies in the cutting-edge unbiased PEC tandem configurations, specifically reviewing recent breakthroughs in coupling PEC CO_2 reduction with the oxygen evolution reaction through water oxidation. By consolidating the latest insights and knowledge, this comprehensive review guides readers through the evolving landscape of advanced PEC technologies. Furthermore, it provides insights into prospective developments in this evolving field, shedding light on the paths toward sustainable energy solutions and climate mitigation.

1. Introduction

The escalating levels of atmospheric carbon dioxide (CO_2) resulting from human activities, primarily the burning of fossil fuels and deforestation, have become a defining issue of our time [1]. The continuous rise in CO_2 concentrations has been a primary driver of global climate change, leading to an array of adverse consequences, including more frequent and severe weather events, rising sea levels, and disruptions to ecosystems [2,3]. As the global community contends with the urgent necessity to mitigate these effects, technologies capable of actively removing CO_2 from the atmosphere while simultaneously providing sustainable energy sources are gaining increasing importance [4].

One promising avenue for addressing this multifaceted challenge is the field of photoelectrochemical (PEC) CO_2 reduction. PEC CO_2 reduction reaction (CO_2RR) harnesses the principles of solar energy conversion and electrochemical reactions to convert CO_2 into high-energy-density fuels as clean energy [5]. This process not only mitigates CO_2 emissions by sequestering carbon in the form of valuable products but also facilitates the high-efficient utilization of renewable energy sources, primarily solar energy [4,6]. By directly coupling solar energy utilization with the electrochemical reduction of CO_2, PEC systems hold the potential to bridge the gap between intermittent renewable energy generation and the production of storable and transportable fuels [7].

Efforts in this field have been driven by a multidisciplinary approach, drawing insights from photochemistry, electrochemistry, and materials science. Extensive efforts have been dedicated to designing PEC systems that are both efficient and scalable, ensuring the practicality of CO_2 conversion to fuels such as syngas, methanol, and ethylene [8,9]. The challenge lies not only in developing novel materials capable of absorbing sunlight and catalyzing CO_2RR but also in optimizing the overall PEC cell architecture and understanding the intricate interplay of factors that influence its performance [10,11].

As the urgency of addressing climate change and transitioning to sustainable energy sources continues to mount, PEC CO_2RR stands as a promising and innovative technology at the intersection of science, engineering, and environment [12]. Many top-notch review articles have comprehensively outlined recent advancements in PEC CO_2RR technologies from diverse perspectives [13,14]. For example, the basic principles and recent advances of PEC CO_2RR have been summarized, especially the state-of-the-art of PEC CO_2RR from the perspective of reaction products, including CO, HCOOH, CH_3OH, CH_4, and C_2 products (Fig. 1) [15]. Meanwhile, a wide variety of photocathodes engineering strategies for CO_2 reduction, such as doping, defect engineering, nanostructuring, cocatalyst, passivation, and heterojunction, have also been outlined in recent review articles [16,17]. Over the last three years,

* Corresponding author.
E-mail address: l.wang@uq.edu.au (L. Wang).

https://doi.org/10.1016/j.apcatb.2024.123707
Received 6 October 2023; Received in revised form 24 December 2023; Accepted 4 January 2024
Available online 7 January 2024

significant and remarkable breakthroughs have arisen in the field of unbiased PEC tandem configurations, with a specific focus on artificial leaves, enabling the integration of CO_2RR with the oxygen evolution reaction (OER) through water oxidation. These recent advancements merit a fresh assessment to spark additional creativity for future innovations. This review provides an up-to-date overview of unbiased PEC tandem setups for CO_2 reduction and conveys our insights on harnessing solar fuels through unbiased PEC CO_2 reduction.

This review centers on the cutting-edge developments in PEC CO_2RR coupled with OER, with a particular emphasis on unbiased PEC tandem configurations. The article commences with a concise introduction to various conceptualizations of PEC CO_2 configurations. It then explores the forefront of PEC CO_2 reduction, starting with a brief overview of fundamental photocathodes featuring significant cocatalysts, and then shifts to the primary subject of this review, namely, unbiased tandem PEC configurations. Finally, we consolidate the state-of-the-art knowledge and provide insights into the evolving trends in advanced PEC technologies for the simultaneous reduction of CO_2 and oxidation of water.

2. Conceptualizations of PEC CO_2 reaction

The foundational principles of photoelectrocatalysis have been comprehensively summarized in the literature [15–17,19–26]. The solid-liquid interface and the photovoltage disparity between the photocathode and the (photo)anode serve as intrinsic driving forces for the separation and transfer of photoexcited charge carriers [21]. This review is primarily focused on exploring various configurations for PEC CO_2 reduction, with a specific emphasis on cutting-edge unbiased setups. Therefore, we first briefly delve into different conceptualizations of configurations for PEC CO_2 reduction, and then discuss how to maximize the PEC CO_2 reduction efficiency.

2.1. PEC CO_2 configurations

The most elemental and straightforward arrangement for PEC CO_2RR involves a photocathode and an anode, augmented by an external bias (Fig. 2**a**). This is necessitated because relying solely on the photovoltage generated by the photocathode rarely enables self-sustaining systems. The use of a photoanode for OER and a dark cathode for CO_2RR is beyond the scope of this article, which may be better addressed in a recent review [27]. An alternative approach is to couple the photovoltage generated by the photoanode, possessing a suitable band structure, with that of the photocathode, thereby enabling the operation of a tandem photocathode/photoanode system without the need for external bias (Fig. 2**b**). Another avenue for harnessing photovoltage (solar energy) exclusively, without requiring additional electricity input, involves combining photovoltaics (PV) and a photocathode (Fig. 2**c**). For optimal soler energy conversion efficiency, it is essential that the photocathode and PV exhibit complementary light absorption properties. There is also a configuration referred to as photovoltaic-electrocatalytic (PV-EC), which consists of a dark cathode and anode in conjunction with PV. While this approach is considered highly promising, it falls outside the scope of photoelectrocatalysis, and is therefore not explored in this discussion.

The aforementioned three configurations all fall under the category of wired setups, characterized by the drawbacks of wiring expenses and ohmic losses. In contrast, wireless PEC configurations have been developed, in which sandwiched PV modules provide power to adjacent photo(cathode) and photo(anode) components (Fig. 2**d**), often referred to as artificial leaves. The incorporation of electrocatalysts for both the cathode and anode is likely to enhance efficiency compared to conventional photoelectrodes, aligning more closely with the concept of wireless PV-EC. However, due to the reliance on solar-powered PV and the unique wireless, standalone, or monolithic structure, it is commonly classified in the literature as either PEC or photochemical artificial leaves. The three configurations in Figs. 2**b**-2**d** represent the contemporary unbiased PEC technologies. As explained earlier, conventional PEC systems rely on an external bias to supply additional photovoltage, given that most photoelectrodes struggle to generate sufficient photovoltage for the reaction and the inevitable overpotential. The incorporation of external bias necessitates both solar energy and electricity, introducing complexity and rendering the system less advantageous for widespread applications. Consequently, unbiased PEC systems, which eliminate the need for electricity and exclusively harness solar energy, are particularly appealing for practical applications due to their

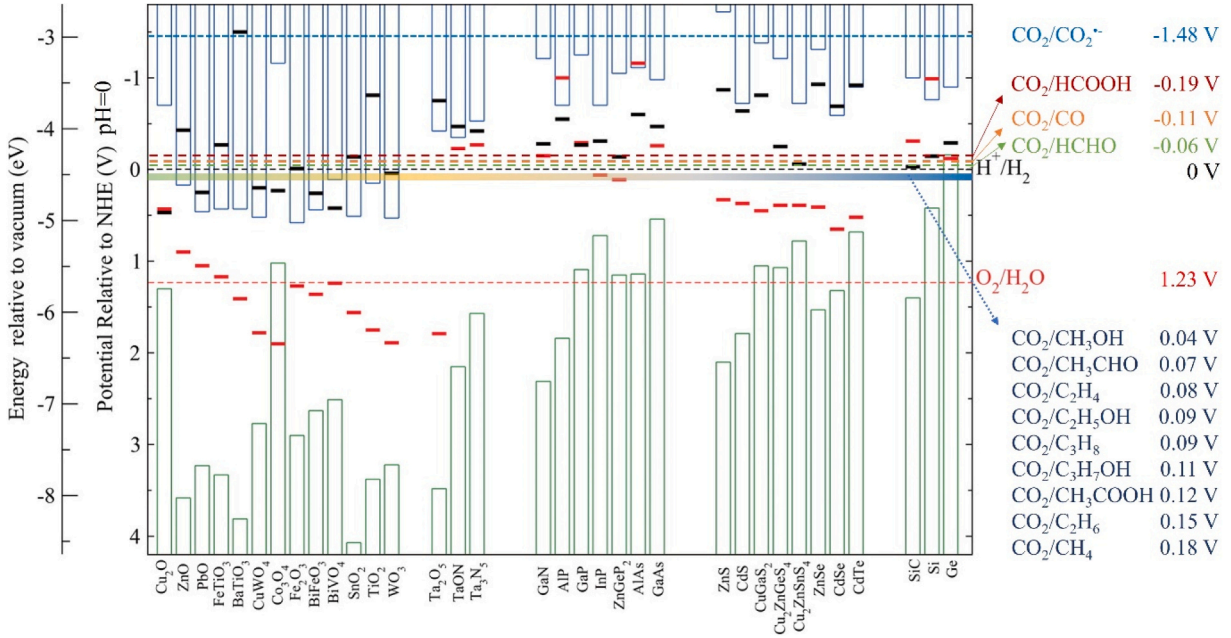

Fig. 1. The bias potentials of various CO_2 reduction reactions, conduction band positions and valence band positions, as well as the calculated semiconductor oxidation and reduction potentials defining the thermodynamic stabilities of semiconductors against photocorrosion. Copyright 2012 American Chemical Society. Adapted with permission from ref [18] with the bias potential data of CO_2 reductions from ref [19].

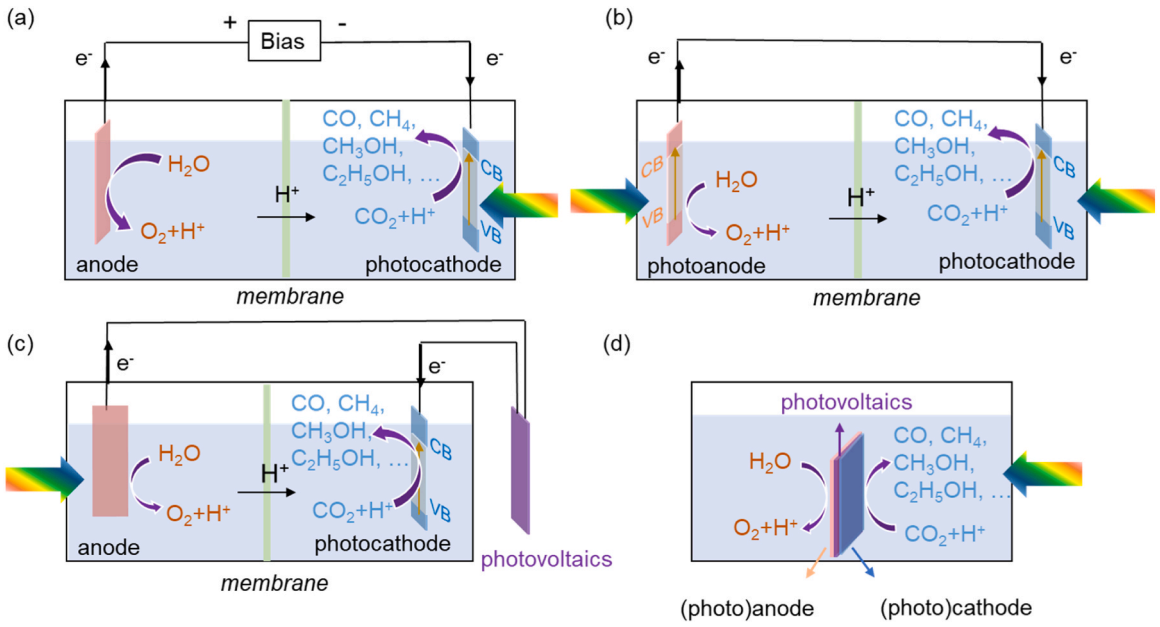

Fig. 2. (a) Common biased PEC CO_2 reduction configuration with photocathode-dark anode. Unbiased PEC CO_2 reduction configurations: (b) Photocathode-photoanode; (c) Photocathode-PV-anode (anode placed at the side of the reactor to avoid light blocking); (d) (Photo)cathode-(photo)anode with sandwiched PV (standalone/monolithic artificial leaves configurations).

simplicity and efficiency [28]. Achieving PV-free unbiased CO_2 reduction with semiconductor photocathodes poses a primary challenge—ensuring sufficient and compatible photovoltage with the (photo) anode. Solar cell/PV materials, also semiconductors, typically have smaller band gaps than those used in PEC reactions. While solar cells/PVs prioritize photovoltage and energy conversion efficiency, semiconductor photoelectrodes must align band positions with the energy potentials of corresponding reactions to avoid recurring high overpotential. Most reported solar cells/PVs exhibit notable water instability, except for silicon, which does not require rigorous encapsulation. Dye-photosensitized solar cells, involving semiconductors with wide band gaps similar to those in photoelectrodes, seem less distinct as a separate PV module. However, due to the use of toxic solvents, dye-photosensitized solar cells are not preferable for practical applications. Consequently, Si solar cells demonstrate dual functionality, although instances of such structures are limited; an example is the a-Si/TiO_2/Au photocathode reported by the Gong group, which incorporates amorphous silicon (a-Si) protected by TiO_2 adorned with grain-boundary-rich gold catalysts [29]. In brief, this review will focus on the three unbiased configurations illustrated in Figs. 2**b**-2**d** as key research highlights for delving into advanced solar-driven technologies for CO_2 reduction.

2.2. *Maximizing PEC CO_2 reduction efficiency*

The fundamental mechanisms of PEC CO_2 reduction have been well summarized in many previous reviews [30]. There elementary steps include light harvest (LH), charge carrier separation and transfer (CST), and surface chemical reaction (CR), with the overall solar-to-chemical efficiency co-determined by these aspects ($\eta_{STC}=\eta_{LH}*\eta_{CST}*\eta_{CR}$). Efficient light absorption is undoubtedly crucial as it lays the foundation for subsequent steps. The separation and transfer of charge carriers are commonly considered the rate-determining "energy pump and delivery" step for overall solar-to-chemical efficiency [31]. This is attributed to their role as the subsequent processes following the conversion of photon energy to chemical energy during photoexcitation, serving as the source of energy driving the final catalytic reactions. To maximize the efficiency of PEC CO_2 reduction, various strategies have been developed to enhance the charge separation and transfer, such as heteroatom engineering, defect engineering, single-atom catalysis, phase engineering, facet engineering, heterojunctions, cocatalysts, localized surface plasmon resonance, surface polarity and so on [16].

On the other hand, the selectivity of end products holds particular significance in CO_2 reduction, given the potential for multiple products with closely aligned energy potentials (see Fig. 1) and substantial variations in demand and economic values among different products. The involvement of CO_2 intermediates is pivotal in shaping the ultimate product species and influencing reaction kinetics. Therefore, optimizing the adsorption of key intermediates during CO_2 reduction is also a crucial aspect in improving the PEC performance. A myriad of strategies has been reported for optimizing the adsorption of CO_2 intermediates. These include adjusting catalyst particle size [32], optimizing the binding energy of CO_2 intermediates with active sites through nanostructuring for various dimensional morphologies or heterostructures, surface engineering incorporating heteroatoms, defects, porosity, acidic/basic sites, and hydrophobic/hydrophilic/amphipathic sites, as well as creating single-atom or double-atom catalytic active sites [16], aligning the energy levels between the photocathode and CO_2 intermediates [23]. As a supplementary tool, in-situ spectroscopies and characterization techniques, such as X-ray Absorption spectroscopy, Infrared spectroscopy, and surface-enhanced Raman spectroscopy, offer potent means to investigate CO_2 intermediates, thereby facilitating further experimental optimization. [33].

3. State-of-the-art PEC CO_2 reduction

In this section, we venture into the leading edge of research on PEC CO_2 reduction. Initially, photocathodes modified by two major categories of cocatalysts are briefly outlined, as photocathode is the most fundamental component of PEC CO_2RR system which directly affects the overall performance (e.g., efficiency, selectivity, stability) and expenses. Our primary focus then shifts to the cutting-edge, unbiased PEC configurations integrating these cocatalyst engineered photocathodes with advanced technologies. Finally, the discussion turns to addressing the stability concerns related to the performance of PEC in CO_2RR. This comprehensive examination offers a state-of-the-art perspective on pioneering research in PEC CO_2 reduction.

3.1. Photocathodes

The photoelectrode is the pillar of photoelectrochemical reaction, and development of advanced PEC technologies heavily replies on the innovation and advancement of photoelectrode. In the past decades, numerous efforts have been made to fabricate photoelectrode of higher efficiency, selectivity, and stability. For PEC CO_2 reduction, it is critical to develop such photocathodes for advancing solar energy conversion to clean fuels. Due to the downward band bending of p-type semiconductor in electrolyte, the photoexcited electrons in the CB are driven to the semiconductor/liquid interface where the reduction reaction occurs [34]. This feature makes p-type semiconductors (p-Si, p-InP, p-NiO, p-Cu_2O, etc.) favourable candidates for solar-driven reduction applications [35]. However, since CO_2RR yields a diverse range of products, achieving desired product selectivity remains a significant obstacle for unaltered semiconductor photocathodes. Adjusting the interactions between intermediates and catalyst surface is frequently accomplished through using cocatalysts to modify the reaction pathway. As some recent review papers have well summarized a wide range of cocatalysts as well as other modification strategies, this review only focuses on the most efficient and applied cocatalysts, including metal and metal complexes, to build the state-of-the-art PEC systems for CO_2RR with unbiased character outlined in Section 3.2.

3.1.1. Metal/Semiconductor Photocathode

Metals have been a common group of cocatalysts for various catalytic reactions, including CO_2RR using photocatalysts or photocathodes. In the past decades, extensive studies have provided knowledge on the selection of metals for specific products, such as the selectivity of various metals towards CO_2 reduction products in aqueous environment (Fig. 3) [20,36,37]. For example, Au has aroused wide interest due to its weak binding to CO* intermediate and thus high selectivity towards CO production from CO_2 reduction as well as surface plasmonic resonance effects beneficial for improving the light absorption of photocathodes [22]. Recently, a photocathode consisting of uniform facet-engineered Au NPs with controllable Au(111)/Au(200) boundaries deposited on p-Si surface was reported to exhibit high CO selectivity up to 82.2% and excellent stability over one week [38]. However, as Au is a rare earth metal with limited availability and usage and the commercial value of CO is much lower than C_2 and C_{2+} species, researchers endeavour to reduce its usage by alloying with non-rare-metals or developing other metal cocatalysts [39]. Due to unique electronic properties, Cu is well known as the only metal capable of catalyzing C–C coupling to C_2 [40,41]. However, the serious competition with hydrogen evolution in aqueous environment, low product selectivity toward a specific carbon product, and low Faradaic efficiency (FE) of metal-cocatalyst based photocathodes is still a long existing great challenge [42]. For instance, interfacing copper nanoparticles to n^+p-Si nanowire photocathodes produced C_2H_4 with FE~25% [43], but it is still a long way towards high selectivity and efficiency to C_2 products through metal cocatalyzed photoelectrodes. Interestingly, a multi-functional synergistic photoelectrocatalytic interface was constructed with intrinsic Au doped TiO_2 as the light harvester, nanotube photonic crystal as optical channels and Cu nanoparticles as cocatalyst, an ultra-high selectivity (98%) towards formic acid and high Faraday efficiency of 82.6% was obtained [44]. The Au greatly extended the light absorption range from UV to visible region, and the Cu cocatalyst promoted the enhancement of PEC CO_2 activity. Instead of focusing on single product from CO_2 reduction, controllable tuning of CO and H_2 as syngas is also highly attractive due to the significance of syngas as a key feedstock in industry. By tuning the interface of metal/oxide (Pt/TiO_2) dual cocatalysts on GaN/n^+-p Si to provide rich multifunctional active sites, a benchmarking solar-to-syngas efficiency of 0.87% was achieved with a high turnover number (TON) of 24,800 and high stability over 10 h and tuneable CO/H_2 ratios with a total unity FE [35]. This provides a new avenue for the design of metal cocatalysts for selective PEC CO_2 reduction.

3.1.2. Metal complexes (molecules)/semiconductor photocathode

Over years, metal complexes (molecules), especially transition metal complexes, have not only been applied in homogenous catalysis, but also been utilized as photosensitizers and/or electrocatalysts for photocatalysts or photoelectrodes to enhance the light absorption and provide active sites [45–47]. Moreover, the structure of the metal complexes can be changed to alter the reaction selectivity, which is of significant importance to multiple electron–proton reduction of CO_2 with a wide variety of potential products, thus low selectivity [24]. Commercial molecular metal complexes have been used in the well-known dye-sensitized solar cells (DSSC), for example ruthenium polypyridyl

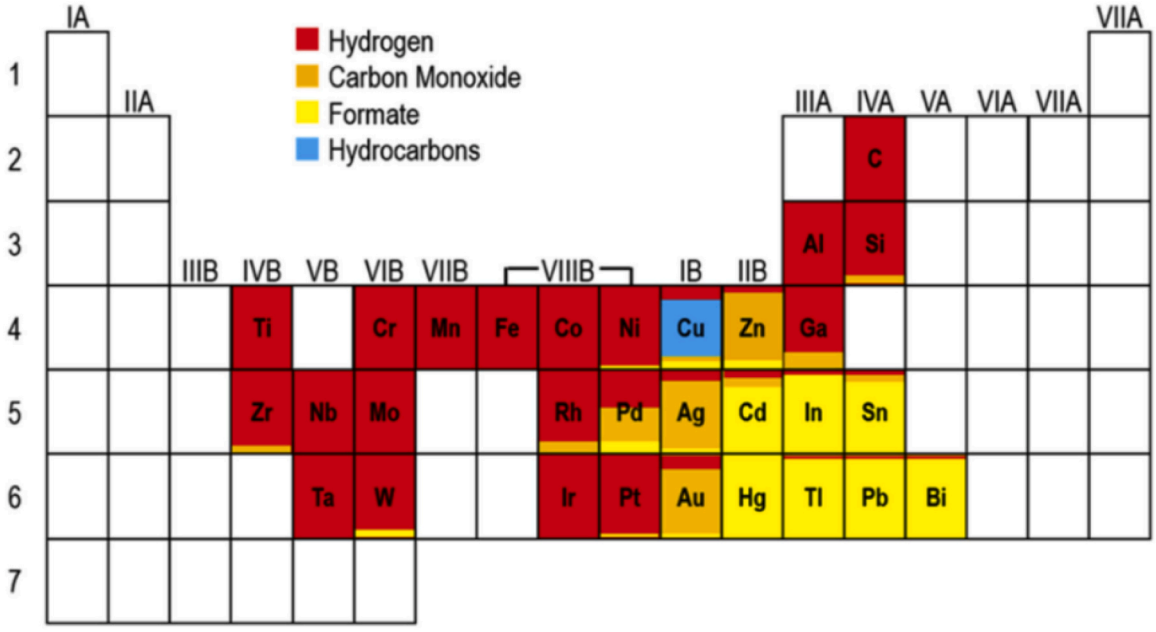

Fig. 3. Primary reduction products in CO_2-saturated electrolytes on different electrodes. Copyright 2015 American Chemistry Society. Adapted with permission from ref [20].

complexes sensitized TiO_2, as TiO_2 is only responsive to UV light due to a large band gap (E_g=3.2 eV). Similarly, dye-sensitized photocathodes have been constructed using wide-band gap semiconductors, molecular reduction catalysts, and photosensitizers, for PEC reduction of CO_2 to CO [48]. Interestingly, a photocathode was reported for CO_2 reduction to CO, which consisted of NiO electrode and a multinuclear supramolecular complex with connected Re(I) and Ru(II) units, Re(I) for reduction reaction and Ru(II) as photosensitizers [49]. However, the molecular components are vulnerable to degradation and serious back electron transfer occurs. Later, a Ru(II)-pyridyl complex covalently bonded TiO_2 nanotube arrays photocathode was demonstrated to exhibit high methanol production for 8 h with high faradic efficiency (63.9%) and excellent stability over 4 reaction cycles [50].

Instead, a recent popular strategy is to build a buried p-n junction by coating a n-type large band gap semiconductor on a p-type narrow band gap semiconductor, allowing broadening light absorption, promoting charge carrier separation, suppressing degradation and thus improving stability [51]. Metal complexes can be used as reduction electrocatalysts on the surface of n-type semiconductor of such photoelectrodes to provide more active sites [52]. Meanwhile, they can also contribute to the light absorption of the hybrid photoelectrodes, especially in visible light range, due to d-d transition and metal to ligand charge transfer.

Binary molecular-semiconductor p-n junctions with a layer-by-layer assembly was reported for PEC CO_2RR (Fig. 4) [51]. n-GaN nanowire arrays were grown on n^+-p^+-n^+ silicon wafers, while molecular assemblies of two photosentisizers phenylene diamine (1,4-bis(azanediyldiacetic acid)benzene (NPhN)) and $Ru(CP)_2$ as well as reduction catalyst RuCt were immobilized on the n-GaN surface. Both the two semiconductors and the molecular photosentisizers formed a p-n junction, and the semiconductors have high hole extraction ability while the molecular assembly has strong electron donating effect. Therefore, the binary p-n junctions finally led to electrons and holes effectively isolated on reduction catalysts and Si respectively. In addition, a two-photon excitation process was realized, enabling enhanced light absorption over a broad wavelength range.

However, as rare metal elements are of high cost and low abundance on earth, they suffer from significant limitations for large-scale applications. A precious-metal-free molecular catalyst-(phosphonated cobalt (II) bis(terpyridine) catalyst, CotpyP) based photocathode was demonstrated for CO_2 reduction [53]. This molecular catalyst was immobilized on the n-type meso-TiO_2 that formed p-n junction with the p-silicon underneath. This photocathode was highly active towards CO and formate production in both hydro-organic and purely aqueous solution, with a TON as high as 381 after 24 h. Since this rare-metal-free molecular based photoelectrode was reported, improvement has been achieved in the following studies using similar strategies with higher selectivity and FE [54]. For example, carbon nanotubes were used as both a support platform for highly dispersed rare-metal-free molecular active sites and an efficient mediator for charge transfer between p-n junction and molecular catalyst in the photocathode, achieving 100% selectivity and 100% FE towards CO_2-to-CO conversion in aqueous media [55]. Excitingly, a rare-metal-free molecular catalyst (cobalt phthalocyanine) based photocathode has been reported to be capable of producing methanol through 6-electron reduction of CO_2, which makes

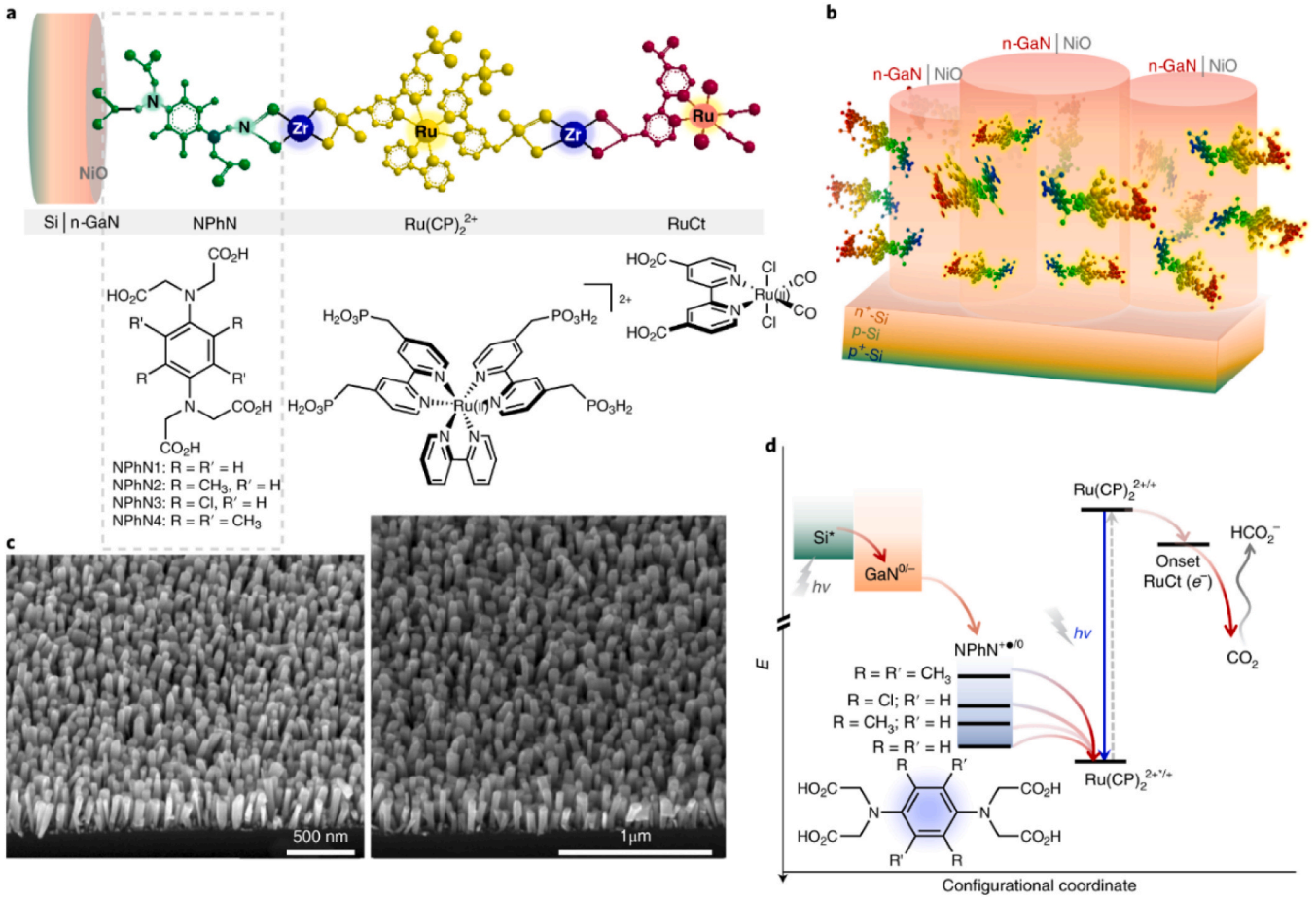

Fig. 4. (a) Layer-by-layer molecular p–n-junction assembly formed by Zr(IV)-phosphonate bridging; (b) Schematic diagram of n-GaN nanowires on the silicon substrate with the surface-immobilized molecular assemblies; (c) Scanning electron microscope images for the pristine n-GaN nanowires; (d) Redox-potential diagram illustrating the relative energy level E, with red arrows showing photoinduced electron transfer direction. Copyright 2019 Springer Nature.
Adapted with permission from ref [51].

it more attractive compared with 2-electron reduction pathways to CO or HCOOH [56].

3.2. Unbiased tandem innovations

In contrast to photocatalysis, which relies solely on light for its energy source, photoelectrocatalysis typically necessitates additional electrical input in addition to solar energy, constituting one of the primary drawbacks of this process. Therefore, numerous attempts have been undertaken to develop unbiased (unassisted/self-biased/self-powered/bias-free) PEC systems. A unique system was reported wherein a self-biased $CuFeO_2$/CuO photocathode, of which the conduction and valence band edges straddle the redox potentials of CO_2 reduction to HCOOH and H_2O oxidation to O_2, worked in junction with Pt dark anode in a two-electrode configuration [57]. This single-absorber self-biased PEC system achieved a solar to chemical (STC) efficiency of 1% towards HCOOH over 1 week despite that self-generated cell potential gradually decreased from ~230 mV to ~170 mV. However, within the literature, the prevalent configurations involve tandem setups featuring two light absorbers, primarily encompassing configurations like photocathode/photoanode, photocathode/PV, and monolithic artificial leaves.

3.2.1. Photocathode/photoanode (PEC/PEC)

The photocathode/photoanode configuration mimics the Z-scheme stepwise excitation in the microorganisms which have two photosystems (PS I and PS II) to generate and maintain the electrons on photocathode and holes on photoanode for the reduction and oxidation half-reactions respectively [58]. The quasi-Fermi level of electrons in the CB of photoanode must be more negative than that of holes in the VB of photocathode, then these electrons and holes can recombine and form a closed-loop circuit. In some studies, two different light sources are applied to photocathode and photoanode to achieve the highest reactivity. However, more studies focus on complementary absorption of solar light (sole light source) using well-matched dual absorbers to maximize the usage of solar spectrum and ensure a compatible magnitude of charge carriers on the two sides. This is one of the most significant challenges in photocathode/photoanode tandem system.

Several metal complex-photocathode/photoanode have been reported. Ru complex immobilised N-doped Ta_2O_5, GaP and p-type InP photocathodes have been integrated with TiO_2/Pt photoanode to perform unbiased reduction of CO_2 to $HCOO^-$ (selectivity over 70%) and oxidation of water in a tandem PEC system [59]. p-type $CuGaO_2$ based RuRe complex-photocathode showed 0.4 eV more positive onset potential for CO_2RR compared with that of RuRe/NiO photocathode, and achieved unbiased CO_2RR and OER fully driven by visible light [60]. However, both these studies utilized two light sources with different wavelength ranges to illuminate the photocathode and photoanode, and thus the light utilization efficiency could be expected to be low. An unbiased tandem PEC cell achieving a STC efficiency of 0.15%, which was assembled using Ru complex-TiO_2/N,Zn-Fe_2O_3/Cr_2O_3 photocathode and $SrTiO_{3-x}$ photoanode for CO_2RR and OER [61]. This work was featured by the complementary light absorption of two photoelectrodes towards sole solar light source, and comparable STC efficiency to photocathode of higher expense, such as InP.

In metal-complex-free tandem system, a n-type semiconductor and p-type semiconductor are used as photoanode and photocathode respectively, due to their band bending features in the electrolyte. Weber and Dignam estimated that simply using two semiconductors of the same band gap (1.4 eV) gave a higher upper limit of solar-to-hydrogen (STH) efficiency than a single semiconductor (16.6%>11.6%), and the STH efficiency can reach 22% using two semiconductors with different band gaps (1.8 eV and 1.15 eV) [62]. Bolton further considered the realistic losses and predict the STH using a contour plot of dual band gaps, and it shows that band gap difference in a certain range gives a higher STH than zero difference (Fig. 5**a**) [63,64]. Based on Lewis group's analysis, the STH efficiency limit for photocathode/photoanode is 29.7% for a pair of light absorbers with band gaps of 1.60 eV and 0.95 eV, which is even higher than that (28.7%) of the high-profile two-junction PV/electrocatalysis (electrolyser efficiency taken as 73%) [65]. Therefore, a large band gap semiconductor (often n-type, e.g., $BiVO_4$, E_g=2.4 eV) often works with a small band gap semiconductor (often p-type, e.g., p-Si, E_g=1.1 eV) to allow the absorption of unabsorbed light in the front semiconductor by the back semiconductor (Fig. 5**a**). In this configuration, the dual-absorber tandem can harness a wider range of solar spectrum light energy compared to a single absorber (Fig. 5**b**) [64].

A tandem system featuring an amorphous Si/TiO_2/grain-boundary-mediated Au photocathode and the well-established $BiVO_4$/FeOOH/NiOOH photoanode was demonstrated for unbiased CO_2RR to syngas and OER under simulated sunlight [29]. The actual unbiased photocurrents (0.22 and 0.24 mA cm^{-2}) for two different ratios of Au turned out to be highly close to the theoretical one (0.25 mA cm^{-2}), with STC_{syngas} efficiencies of 0.27% and 0.29%, respectively. More recently, multiple-pixel devices were demonstrated as an innovative design principle for PEC systems, of which the photocathodes integrating a BiOI light absorber into a robust, oxide-based architecture with conductive graphite epoxy encapsulant with depositing $Cu_{92}In_8$ electrocatalysts [66]. The BiOI|GE|$Cu_{92}In_8$ photocathode–$BiVO_4$ photoanode tandem system achieved unbiased syngas production from CO_2 reduction, despite low solar-to-H_2/CO efficiencies of 0.042%/0.045%.

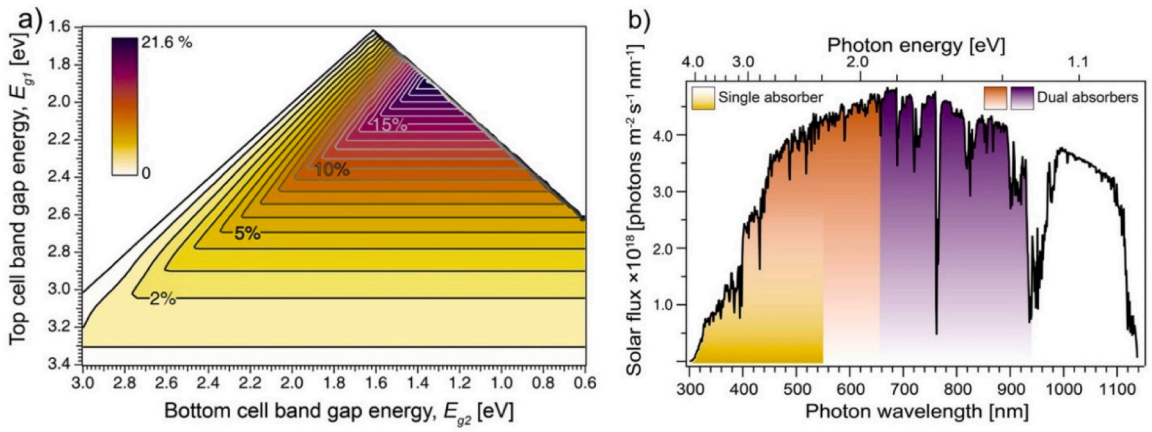

Fig. 5. (a) Contour plot showing the maximum predicted STH efficiency (η_{STH}) of dual-absorber system considering a total loss of 2.0 eV (U_{loss}); (b) Light absorption of single absorber and dual absorbers. Copyright 2013 American Chemistry Society.
Adapted with permission from ref [64].

In the context of the PEC/PEC unbiased system, the significance of not only the photocathode for CO_2RR but also the photoanode for OER cannot be overstated, as it significantly influences the overall system efficiency. Existing literature on unbiased PEC/PEC systems for CO_2RR has employed (pristine or cocatalyst-loaded) semiconductors such as (Pt-)TiO_2 [59,67], (NiOOH/FeOOH)$BiVO_4$ [29,66], reduced $SrTiO_3$ [61] and (CoO_x-)TaON [60] for the OER half reaction. Among these, $BiVO_4$ stands out as a commonly used semiconductor for PEC OER, owing to its favorable properties in catalyzing water oxidation to O_2. Several comprehensive review papers have consolidated insights into photoanodes, detailing approaches to enhance their light absorption capabilities, charge separation and transfer, and surface reaction rates [68–71]. While PEC/PEC unbiased systems for CO_2RR are currently in their early stages of development, future research endeavors are expected to capitalize on the most efficient photoanodes to advance the field.

3.2.2. PEC/PV

Illuminated PV generates voltage, which can work as the source of external bias for photocathode. Like direct water electrolysis, it is not only of scientific interests but also promising in cost reduction and energy saving to couple PV with photocathode for CO_2RR with light as the only energy input [67,72]. Typically, the photocathode is positioned in front of the PV module from the direction of illumination to maximize light absorption, given its lower light-absorption capacity compared to the PV module due to a wider bandgap. The photogenerated holes in photocathode recombine with the photogenerated electrons on PV, and the electrons of the counter electrode transfer to PV and recombine with the left photogenerated holes on PV [73].

Although the theoretical upper limit of photocathode/photoanode is higher than that of PEC/PV tandem cell, the reported PEC/PV systems outperform the photocathode/photoanode. In PEC/PV system, the energy efficiency is determined by both PV and PEC. III-VI group, Si junctions, or perovskites have often been used as the PV component, among which the III-VI PVs are at least an order of magnitude more expensive than the Si single-junction cell, the Si PVs have been dominating the solar market after successful commercialization, and the perovskite PVs are attractive for low-cost and high adjustability [74]. Due to Shockley–Queisser limits, the theoretical solar-to-electricity efficiency of the widely known Si is ~29.8%, while the highest experimental efficiency for various Si cells is 27.6% to date [75]. Perovskite tandem has exhibited a higher solar-to-electricity efficiency up to 33.7% so far [76], and there is still much room to be further improved. Therefore, researchers working on PEC/PV for CO_2RR have been improving the overall efficiency by developing more efficient photocathode and combining more efficient PV modules. A tandem PEC/PV cell consisted of Au decorated triple-layered ZnO@ZnTe@CdTe core-shell nanorod array photocathode with common perovskite $CH_3NH_3PbI_3$ solar cell was constructed for unbiased PEC CO_2RR [77]. This tandem device achieved a steady solar-to-CO efficiency over 0.35% and overall STC efficiency above 0.43%. As shown in Fig. 6, double-junction $CH_3NH_3PbI_3$ perovskite solar cells were combined with Si photocathodes integrated with Ag-supported dendritic Cu catalyst, forming a self-powered PEC/PV tandem system for CO_2RR [78]. It was a great breakthrough that the system maintained over 60% FE to hydrocarbon and oxygenate products (mainly C_2, C_3 species) for several days, with record high efficiencies of 0.5% for solar to high-value-added C_2 and C_3 products and 3.5% for all products.

The limited research on PV-PEC monolithic systems presents a notable gap in our understanding of this technology. One primary barrier is the complex integration of PV and PEC components into a single monolithic system. The challenges include optimizing material compatibility, achieving complementary light absorption and efficient charge transfer between PV and PEC components, and maintaining overall system stability. To further advance in this technology, researchers could explore innovative material combinations that enhance both the PV and PEC aspects. This may involve developing new materials with improved durability, corrosion resistance, and tailored band structures. Additionally, optimizing the interface between PV and PEC components to maximize charge transfer efficiency and exploring advanced fabrication techniques could contribute to overcoming existing barriers.

3.2.3. Monolithic artificial leaves

In 2011, Nocera group developed solar water-splitting cells comprising PV and reduction and oxidation catalysts for water splitting in both wired and wireless configurations [79]. Although the wireless configuration showed a lower efficiency of 2.5% compared with that (4.7%) of a wired configuration under simulated solar light due to significant Ohmic voltage losses, it has attracted increasing attention as wireless configuration greatly simplifies the design of the device and reduces the costs [80]. While the efficiency is likely to be lower than the wired counterpart, the monolithic artificial leaves can offer irreplaceable advantages from the perspectives of manufacturing, expense, and application scenarios.

The first artificial leaf for CO_2RR was fabricated in 2013, although the solar conversion efficiency was lower than that for water splitting as high-efficiency three-junction a-Si and electrocatalysts were used in Nocera's work. Both wired (photocathode/photoanode) and wireless (artificial leaves) devices with RuCP/InP photocathode irradiated by visible-infrared light and reduced $SrTiO_3$ as photoanode illuminated by simulated solar light, achieving high solar conversion efficiency of 0.14% (wired) and 0.08% (wireless) [81]. Then, a record high solar conversion efficiency of 4.6% of PV-EC artificial leaves (IrO_x/si-Ge-jn/carbon cloth/p-RuCP) was achieved for reduction using water as electron donor under simulated solar light (Fig. 7**a**) [82]. The significant

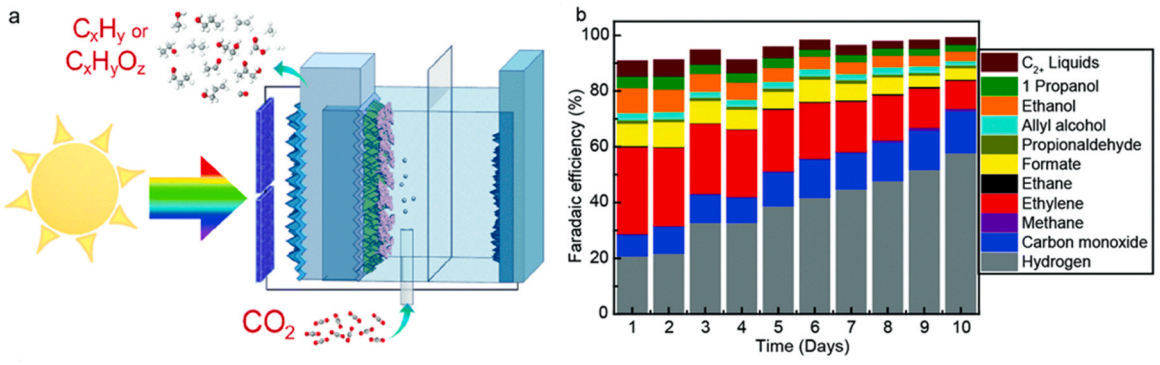

Fig. 6. (a) Schematic diagram of PEC CO_2RR performed in a two-electrode configuration in tandem with two series-connected semi-transparent perovskite solar cells; (b) CO_2RR products over time. Reproduced from ref [78] with permission. Copyright 2019 Royal Society of Chemistry.

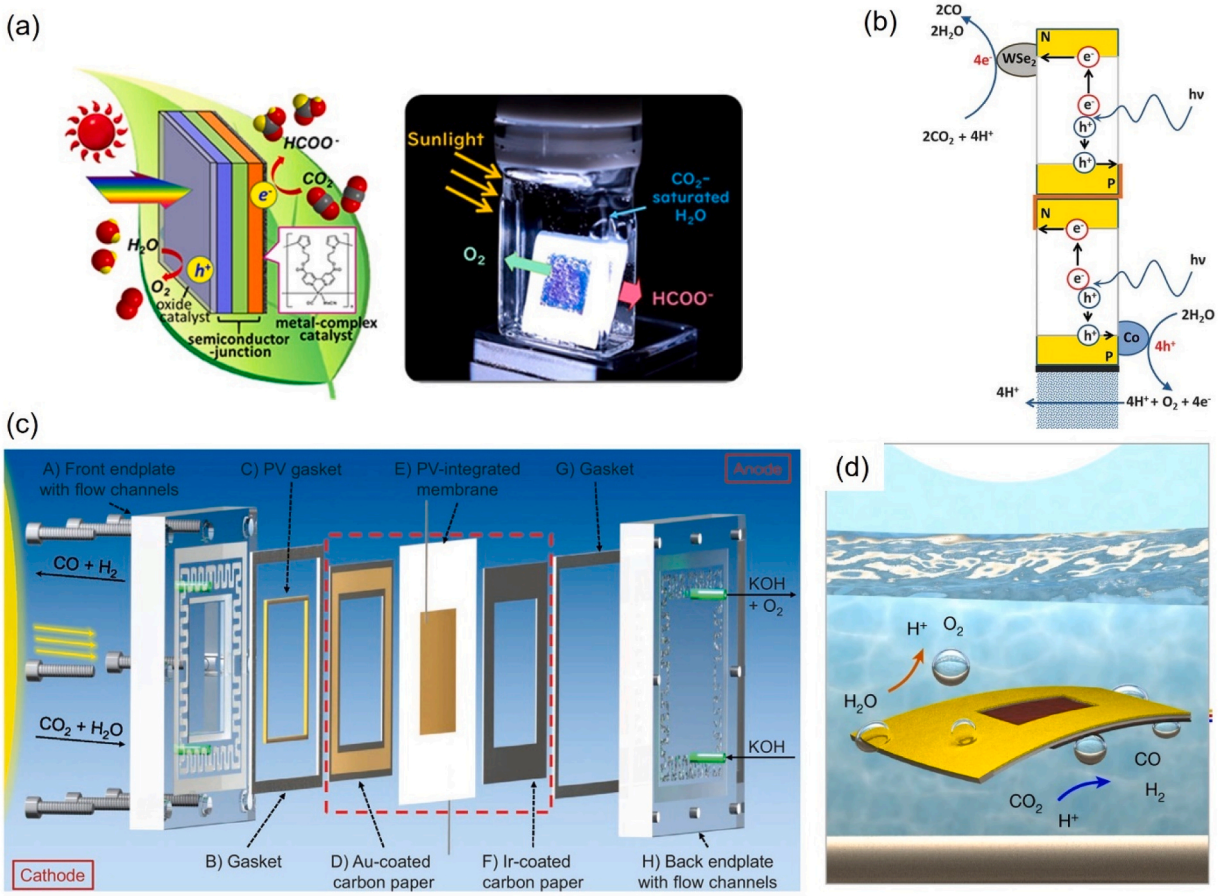

Fig. 7. Schematic diagrams of an (a) artificial leaf that works in a single-compartment reactor; Copyright 2022 American Chemical Society. This publication is licensed under CC-BY-NC-ND 4.0. Copyright 2016 American Association for the Advancement of Science. Copyright 2021 Wiley-VCH GmbH. Copyright 2022 Springer Nature.
(a) Adapted with permission from ref [11]; (b) artificial leaf that works in a two-compartment reactor. (b) Adapted with permission from ref [83]; (c) monolithic flow-cell PEC device enclosing PIM. (c) Adapted with permission from ref [85]; (d) light-weight artificial leaf for syngas production. (d) Adapted with permission from ref [87].

improvement of STC efficiency attributed to enhancing the efficiencies of both PV and catalysts. Interestingly, another PV-EC artificial leaf utilizing a cathode consisted of electrocatalyst WSe_2 in ionic liquid (50 vol% EMIM-BF_4 in water), a Co(II) oxide/hydroxide anode for OER in KPi solution, and a sandwiched three-junction a-Si as PV was demonstrated for CO_2 reduction to CO coupling with OER [83]. Different from the other reported artificial leaves that were operated in a single compartment, this monolithic device worked in two compartments with ionic liquid in the cathode compartment significantly enhancing the efficiency (Fig. 7**b**). Given that the efficiency of the PV module did not exceed 6%, it was indeed a significant accomplishment that the artificial leaves exhibited a substantial STC efficiency of ~4.6%. Another prototype of PV-EC artificial leaves for CO_2RR utilized gas-diffusion electrodes with a design similar to commercial electrolysers, featured by flow-cell configurations and a bipolar membrane separated compartments operating under different electrolytes [84]. It achieved an operation current density of 5.0 mA cm^{-2} under simulated solar illumination, with a solar-to-syngas efficiency of 4.3% and tuneable CO:H_2 ratios (0.5–5) favourable for different application scenarios. A unique PV-integrated-membrane (PIM) based flow-cell artificial leaf, which resembles the membrane electrode assemblies (MEA) in commercial electrolysers, achieved close contact with electrocatalysts and gas-diffusion layers (Fig. 7**c**) [85]. Excitingly, this PIM, MEA-style PV-EC artificial leaf achieved the highest STC efficiency over 10%, due to a synergy of the novel device design, highly active electrocatalysts and high-efficient PV.

Lately, Reisner group published findings on three artificial leaf systems designed for CO_2RR and OER. These systems employ either perovskite-driven molecular catalysts or dual-metal electrocatalysts in conjunction with $BiVO_4$ photoanodes. Although the STC efficiencies of these systems are not comparable with the studies above, they demonstrated solar to syngas conversion under low solar irradiation (0.1 sun) in neutral pH environment [86], lightweight floating artificial leaves for open-water applications that showed promise for up-scaling from 1.7 to 100 cm^2 (Fig. 7**d**) [87], and exploration towards production of multi-carbon alcohols with a total FE of 7.5% and STC of 0.31% towards ethanol and n-propanol [88].

In recent years, the integration of semi-artificial PEC systems, which combine natural enzymes with artificial semiconductors as photoelectrodes, with PV modules result in the emergence of a subcategory known as semi-artificial leaves within the realm of artificial leaves. Several groups focus on semi-artificial-PEC cathodes, which directly immobilize the enzymes on semiconductor photoelectrode instead of dispersing in electrolyte and working in junction with redox mediator [89,90], for CO_2 reduction. Semi-artificial-PEC systems are highlighted to be biomimetic via ‘‘reverse combustion’’ in order to generate organic carbon [91]. Due to the high catalytic activity and chemical selectivity of enzymes for CO_2RR in mild conditions, researchers have also attempted to couple enzymes with photoelectrocatalysis for CO_2RR [91]. Weaver group first reported enzyme-PEC CO_2 reduction to formate, being the pioneer of semi-artificial-PEC technologies, with p-type InP as the photocathode, methyl viologen as the redox mediator,

and formate dehydrogenase as the biocatalyst [92]. There are no doubts that unbiased semi-artificial-PEC systems are more realistic than the biased ones, considering the solar-driven feature of natural synthesis and the stability of the enzymes. Park group showcased a groundbreaking achievement of by presenting the first semi-artificial leaves —a wireless solar-driven semi-artificial PEC system, which successfully achieved CO_2RR without bias, using water as an electron source [93]. The photocathode was fabricated by interfacing formate dehydrogenase onto TiO_2-coated $CuFeO_2$/CuO mixed oxide, further forming a wireless Z-scheme with a well-established FeOOH|$BiVO_4$ photoanode (Fig. 8**a**). The total photovoltage (ca.1.9 V, ca.1.0 V from $BiVO_4$ plus ca.0.9 V from $CuFeO_2$/CuO) was larger than the thermodynamic potential difference between CO_2RR and OER (1.272 V). Due to the decomposition of unstable $CuFeO_2$, the tandem cell exhibited a low FE_{HCCOH} of 33.5% and low STC_{HCOOH} of 0.008%. A different semi-artificial leaf was illustrated, featuring a semi-artificial photocathode comprising perovskite, inverse opal TiO_2, and W-dependent formate dehydrogenase (FDH). This photocathode was connected to a $BiVO_4$ photoanode, enabling the accomplishment of unbiased PEC CO_2RR and OER (Fig. 8**b**) [94]. The semi-artificial photocathode provided an optimal local enzyme environment via the electrolyte solution and achieved an unprecedented current density (-5 mA cm^{-2} at $+0.4$ V vs. reversible hydrogen electrode (RHE)) and a more positive onset potential. A high 0.8% STC_{HCOOH} efficiency, which was 10-fold improved performance compared with Park's work, and a higher FE of 83% was obtained.

With the advancement in unbiased tandem PEC cell technology, it is beneficial to assess various configurations to guide future research directions. The photocathode-photoanode configuration stands out as the simplest and most cost-effective choice for photoelectrode fabrication and integration [95]. However, it necessitates precise alignment of semiconductor band structures and faces challenges in achieving the theoretical efficiency range of 20–30% due to inherent issues such as non-ideal photoelectrode properties, Ohmic losses, and photoelectrode degradation. In contrast, PEC/PV configurations are generally regarded as the most efficient and promising option among PEC technologies, especially in terms of efficiency and the availability of commercial photovoltaic components. Nevertheless, this configuration suffers from higher costs and lower stability in the photovoltaic component, despite recent reductions in photovoltaic prices and shorter energy payback periods, which now stand below 2.5 years [96,97]. Both wired configurations mentioned above share similar advantage of avoiding reverse reaction due to the necessity for two compartments and disadvantage of wiring expenses.

On the other hand, wireless configurations, namely monolithic

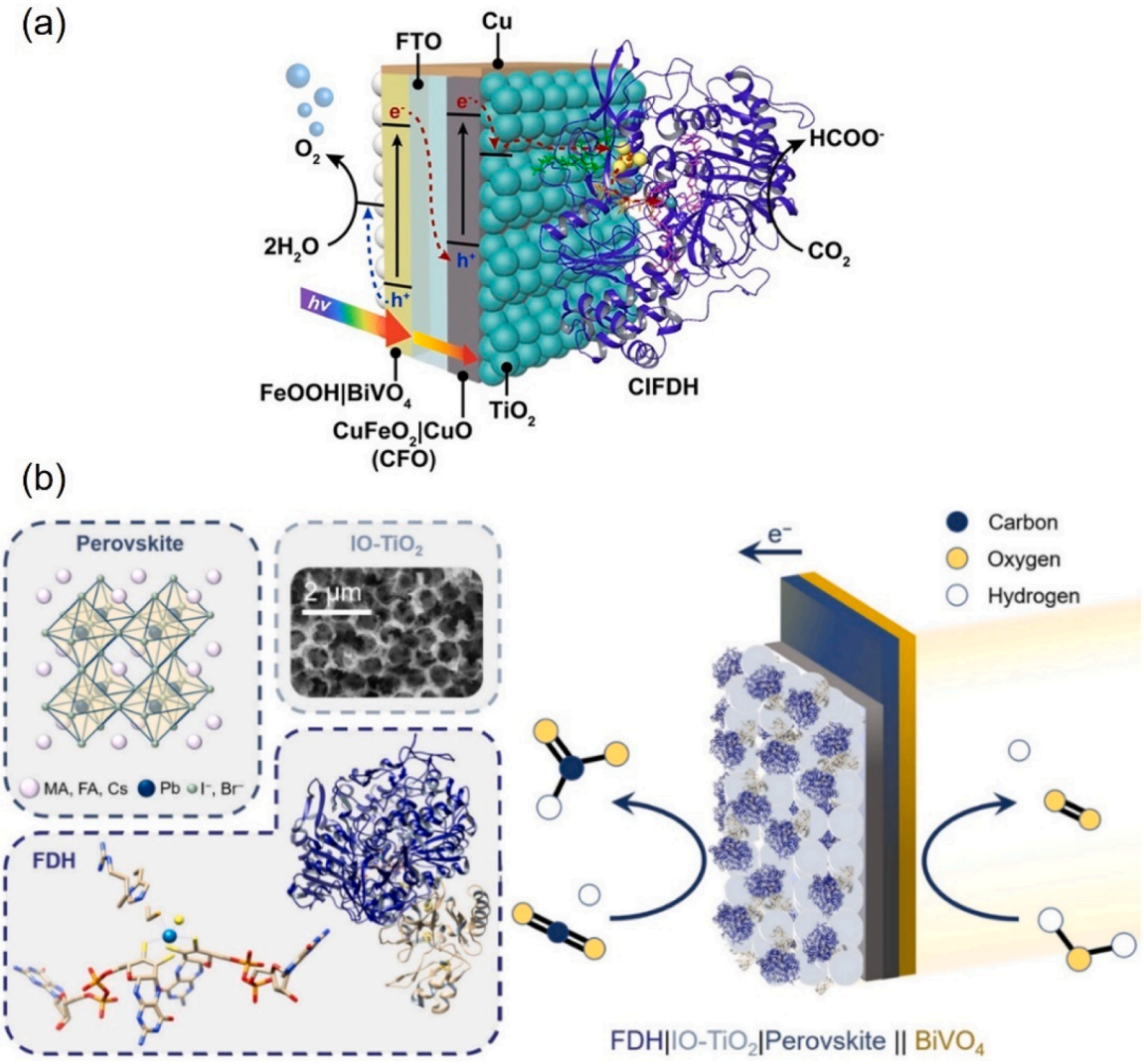

Fig. 8. Schematic illustration of (a) FeOOH|$BiVO_4$||ClFDH–TiO_2|CFO and (b) FDH|IO-TiO_2|perovskite||$BiVO_4$ semi-artificial leaves for unbiased biocatalytic CO_2 conversion into formate using water as an electron donor. Copyright 2020 Wiley-VCH. (b) Copyright 2021 Wiley-VCH.
(a) (a) Adapted with permission from ref [93]. (b) Adapted with permission from ref [94].

artificial leaves, do not require wiring connections and thus materials cost reduction due to their sandwiched structure [98]. While the current efficiencies attained by artificial leaves are relatively modest, their inherent simplicity akin to natural photosynthesis and their wide-ranging potential applications in various real-world scenarios, such as large-scale systems, portable devices, and floating platforms, position them as the ultimate aspiration in the realm of artificial synthesis. Among this category, semi-artificial leaves offer an added benefit of high selectivity due to the integration of enzymes. However, all these wireless configurations still lag behind PEC/PV setups in terms of reaction kinetics and efficiency [64]. Additionally, they exhibit reduced stability over extended periods due to structural degradation and catalyst decay, with semi-artificial leaves being particularly susceptible to suppression or damage in unfavorable environmental conditions, such as variations in pH levels or exposure to high salt concentrations [99, 100]. A brief comparison of the three unbiased PEC configurations for CO_2 reduction is depicted in Fig. 9.

Improving the performance of unbiased PEC systems, whether used for PEC/PEC, PEC/PV, or artificial leaves, involves optimizing various aspects to enhance the efficiency of light absorption, charge separation, and conversion of solar energy into electrical or chemical energy. Here are specific approaches tailored to each of these categories:

PEC/PEC: (1) enhancing the band structure and light absorption compatibility of photoanode and photocathode; (2) optimizing the co-catalysts on both photoelectrodes to ensure compatibility for the desired reactions; (3) balancing the rates of anodic and cathodic reactions to prevent overpotential losses and maximize overall system efficiency; (4) considering the introduction of redox mediators in the electrolyte to enhance charge transfer between the photoanode and photocathode.

PEC/PV: (1) exploring more efficient photocathodes with compatible band gap, light absorption capability, and electronic structures with the PV module; (2) optimizing the cocatalysts on the photocathode for CO_2RR and using a suitable anode for OER to improve the charge transfer kinetics; (3) taking advantage of the recent research breakthroughs in solar cell, such as multi-junction solar cell devices; (4) designing novel device architectures for better alignment of the photocathode and PV, such as integrated tandem cells or 3D structures, to improve light harvesting and charge collection.

Artificial leaves: (1) optimising the interfaces between multiple layers in the monolithic structure for better charge transfer; (2) enhancing the band structure and light absorption compatibility of the photocatalytic materials (if any) and the PV module; (3) exploring configurations of multi-junction monolithic devices from new perspectives, for instance, orientation, thickness, weight, or shape; (4) improving the encapsulation techniques to protect against degradation of the materials (especially the PV module or electrode) or dissociation of the interfaces.

Table 1 serves as a concise summary of representative PEC configurations tailored for the coupling of CO_2RR with OER. The encapsulated information includes crucial details on reaction conditions and system performance and stability, offering a comprehensive perspective to facilitate a thorough analysis of the state-of-the-art in this field.

3.3. Stability mitigation

Stability is a prominent concern in PEC systems, as evidenced by the prevailing trend in the literature indicating a gradual decrease in performance over extended periods, typically spanning hours or days (Table 1). Addressing this issue is crucial for the advancement of PEC technology. To mitigate the observed performance decline, several potential strategies can be considered.

1. Material selection and coating: Explore the use of stable and corrosion-resistant materials for the electrodes. Protective coatings or surface modifications can also be employed to enhance the durability of the materials in the harsh PEC environment.
2. Electrolyte optimization: Investigate electrolyte compositions that contribute to system stability. The choice of electrolyte can significantly impact the corrosion rates and overall stability of the PEC system. Optimizing the electrolyte parameters may lead to improved long-term performance.
3. Operational conditions: Examine the operational parameters such as temperature, pressure, and flow rates to identify optimal conditions for stable performance. Careful control of these factors can contribute to mitigating degradation over time.
4. System design and engineering: Consider modifications to the overall system design to enhance stability. This could involve improved cell configurations, better sealing mechanisms, or the integration of feedback control systems to maintain optimal operating conditions.
5. Monitoring and maintenance: Implement regular monitoring protocols to detect performance degradation early on. This proactive approach allows for timely intervention or maintenance to address issues before they significantly impact the system's stability.
6. In-depth analysis of degradation mechanisms: Conduct a detailed analysis of the degradation mechanisms. Understanding the root

	Photocathode-photoanode	Photocathode-photovoltaics	Monolithic artificial leaves
Advantages	❑ Relatively low cost ❑ Facile fabrication integration ❑ Avoid reverse reaction	❑ High realistic efficiency ❑ Some PVs commercially available ❑ Avoid reverse reaction	❑ Simple operation ❑ No wiring requirements ❑ Relatively high selectivity (semi-artificial leaves) ❑ Broad applicability
Disadvantages	• Strict matching of band structures • Large gap between theoretical and realistic efficiencies • Wiring expenses	• High cost • PV stability • Wiring expenses	• Large gap between theoretical and realistic efficiencies • Sensitive to environment (semi-artificial leaves) • Stability issue

Fig. 9. Comparison of the advantages and disadvantages of different unbiased tandem PEC cells for CO_2RR and OER.

Table 1
Representative PEC configurations for CO_2RR coupling with OER.

PEC configurations	Photocathode	(Photo) anode	Photovoltaic	Reaction conditions	Performance	Stability	Reference
PEC	$CuFeO_2$/CuO	Pt	NA	1 sun (AM 1.5 G), CO_2-purged bicarbonate (0.1 M)	HCOOH ~60 μmol in 24 h (2.5 μmol h^{-1}) FE ~90% STC 1–1.2% in 5 h and then stabilized to ~0.7% in the following hours	Cell potential gradually decrease over 7 days with continuous production of HCCOH (250 μmol)	[57]
PEC	p-type CuO/Cu_2O microchannel nanorod arrays	Pt	NA	70 mW cm^{-2}, AM 1.5 G, CO_2 saturated 0.1 M $NaHCO_3$, under − 0.3 V vs Ag/AgCl, continuous	C_2H_5OH: ~7.2 C_3H_7OH: ~2 CH_3OH: ~1 (mmol cm^2 h^{-1})	Photocathode stability less than 4 h	[101]
PEC	Pt-TiO_2/GaN/n^+-p Si	Pt	NA	300 W xenon lamp (800 mW cm^{-2}, ~8 suns), CO_2-saturated 0.5 M $KHCO_3$ solution (pH 7.5)	Tuneable CO:H_2 ratio by changing potential, TON 24,800, highly positive onset potential of + 0.47 V (underpotential of 580 mV to the CO_2/CO equilibrium potential at −0.11 V), FE_{CO}= 78%, STC_{syngas}= 0.87%	Stable in 10 h	[35]
PEC	a-Si/TiO_2/Au	Pt	NA	1 sun (AM1.5), CO_2-saturated 0.1 M $KHCO_3$	Tuneable CO:H_2 ratio by changing potential, Max FE_{CO}= 50%, CO mass activity 180 A g^{-1} Au at − 0.1 V_{RHE}, applied bias photon-to-current efficiency 0.42%	Stable in 10 h	[29]
PEC	one dimensional wedged N-doped CuO	Pt	NA	Xe lamp with a band-pass filter (λ ≥ 420 nm, 100 mW cm^{-2}), CO_2-saturated 0.1 M $KHCO_3$	Methanol production 3.60 mmol L^{-1} cm^{-2} and current efficiency 84.4% at − 1.2 V_{SCE}	Nearly linear production of methanol in 6 h	[102]
PEC	Chorine modified Cu_2O|ZnO	Pt	NA	Xe lamp with a filter (λ > 420 nm, 239 mW cm^{-2}), CO_2-saturated 0.1 M $KHCO_3$	high selectivity of 88.6% for CH_4 at − 0.6 V_{RHE}	Nearly constant photocurrent density in 5 h	[103]
PEC	p-type Cu/Cu_2O nanobelt arrays	Pt	NA	Blue LED light (435-450 nm), 0.1 M $KHCO_3$ Solution, − 2.0 V vs Ag/AgCl	C_2H_4: 32.69% current efficiency CH_4: 0	Photocathode stability less than 30 min	[104]
PEC	CuN_x|CuO	Pt	NA	1 sun (AM1.5), CO_2-saturated 0.1 M $KHCO_3$	FE_{C2}= 15.2% − 1.0 mA cm^{-2} at 0.2 V_{RHE}	FE towards ethanol slightly decreases while the photocurrent density slightly increases in 5 h	[105]
PEC	p-type B-doped g-C_3N_4	Glassy carbon electrode	NA	1 sun (AM 1.5 G), 0.5 M $NaHCO_3$ solution (pH = 7.3)	Onset potential ~0.15 $V_{Ag/AgCl}$ (pH=7.3), FE_{EtOH}= 78%	NA	[106]
Metal complex-PEC	Si|mesoTiO$_2$|CotpyP	Pt	NA	E_{app} = −1.0 $V_{Fc+/Fc}$ for MeCN:H_2O mixtures; 1 sun (AM 1.5 G); CO_2-saturated 0.1 M $TBABF_4$ in MeCN:H_2O or 0.1 M $KHCO_3$	Photocurrent − 90μA cm^{-2}, FE= 77%@ 0 $V_{Fc+/Fc}$, TON_{CO}= 334, TON_{HCOO-}= 48, TON_{H2}= 246 in 0.1 M $TBABF_4$, 6:4 v:v MeCN:H_2O; FE= 63% @ 0 V_{RHE}, TON_{CO}= 9, TON_{HCOO-}= 11.8, TON_{H2}= 35.6 in 0.1 M $KHCO_3$	91% photocurrent retained after 24 h in 0.1 M $TBABF_4$, 6:4 v:v MeCN:H_2O; 8% photocurrent retained in 0.1 M $KHCO_3$	[53]
Metal complex-PEC	Si-TiO_2-APTES-GO/CoPc	Graphite rod	NA	300 W Xenon lamp with a UV cutoff filter (>400 nm), 150 mW cm^{-2}, 0.1 M CO_2-saturated aqueous $KHCO_3$	onset potential − 0.36 V_{RHE}, peak turnover frequency of 0.18 s^{-1}, peak CO selectivity of 86% at − 0.28 V and peak MeOH selectivity of 8% at − 0.62 V	Under 1 sun, E = −0.19 V, FE_{CO}= 86% stable in 6 h and slightly decrease over 6 h; E = −0.62 V, FE_{MeOH}= 6% in the first hour and then decreased	[56]

(*continued on next page*)

Table 1 (*continued*)

PEC configurations	Photocathode	(Photo) anode	Photovoltaic	Reaction conditions	Performance	Stability	Reference
Metal complex-PEC/PEC	N-Ta_2O_5 or GaP or InP/ Ru-complexes	TiO_2-Pt	NA	Xe lamp, $\lambda > 400$ nm, 1 sun (AM1.5), no external bias, 10 mM CO_2-saturated $NaHCO_3$ solution	0.03 − 0.04%	NA	[59]
PEC/PEC	p-GaP	n-TiO_2	NA	Unfiltered Hg lamp, 0.1 M Li_2CO_3	Constant photocurrent density 2.1 mA cm^{-2} on photocathode CH_3OH FE 60%	Over 16 h	[67]
PEC/PEC	$RuRe/CuGaO_2$	CoO_x/ TaON	NA	Photocathode: $\lambda_{ex} > 460$ nm using a 300 W Xe lamp; Photoanode: $\lambda_{ex} > 400$ nm using a 300 W Xe lamp $NaHCO_3$ saturated with CO_2 (pH 6.6)	2 h, FE(CO+H_2)= 72%, CO 232 nmol and 311 nmol H_2; FE_{O2}= 70%, O_2 266 nmol	NA	[60]
Metal complex-PEC/PEC	TiO_2/N, Zn-Fe_2O_3/Cr_2O_3-Ru complex	n-$SrTiO_{3-x}$	NA	1 sun (AM1.5), no external bias, 0.1 M $KHCO_3$	Photocurrent: 102 μA cm^{-2} HCOOH: 1.55 (μM cm^{-2}) FE= 79% CO: 0.31 (μM cm^{-2}), FE= 16% H_2: 0.12 (μM cm^{-2}), FE= 6% STC 0.15%	> 3 h	[61]
PEC/PEC	a-Si/TiO_2/Au	$BiVO_4$/ FeOOH/ NiOOH	NA	1 sun (AM1.5), shone from the $BiVO_4$ side, photocathode in CO_2-saturated 0.1 M $KHCO_3$, photoanode in 1 M KBi	unbiased photocurrent 0.24 mA cm^{-2}, STC_{syngas}= 0.29%	Stable in 2 h	[29]
PEC/PEC	BiOI|GE| $Cu_{92}In_8$	$BiVO_4$	NA	1 sun (AM1.5), 0.5 M $KHCO_3$ solution, pH 7.4, under CO_2	onset voltage − 0.15 V, CO: H_2 = 3.7:1 in 2 h, STH 0.042% and STC_{CO} 0.045% in 12 h without external bias	Photocurrent gradually decrease over 72 h	[66]
PV-PEC	p-GaP	carbon rod	Si	Unfiltered Hg lamp, 0.1 M Li_2CO_3	38 h HCHO: 2 mM CH_3OH: 0.3 mM	Current gradually decreased from 0.05 mA to 0.01 mA in 38 h	[67]
PV-PEC	WO_3	Cu_xO	Dye sensitized TiO_2	1sun (AM 1.5 G), 0.1 M bicarbonate	5 h STC_{CO}= 2.5%, STH= 0.7%, STC_{HCOOH}= 0.25%	NA	[107]
PV-PEC	ZnO|ZnTe| CdTe|Au	CoCi|Ni foam	$CH_3NH_3PbI_3$ perovskite	1sun (AM 1.5 G), 0.5 M $KHCO_3$	3 h CO 30.10 μmol, H_2 10.10 μmol; photocurrent density ≈ 0.8 mA cm^{-2}, FE_{CO}= 88.92%, $selectivity_{CO}$= 74.86%	Photocurrent gradually decrease over 3 h	[77]
PV-PEC	$p^{\pm}$/n-Si/$p^{\pm}$| TiO_2|CuAg	IrO_2 or CoPi	Double-junction $CH_3NH_3PbI_3$ perovskite	1sun (AM 1.5 G), 0.1-0.5 M $KHCO_3$	STC_{C2+C3}= 1.5% $STC_{all\ products}$=3.5%	Stable over 10 h; maintained over 60% FE towards C_2 and C_3 products for several days	[78]
Monolithic Artificial leaves	InP-RuCP	reduced $SrTiO_3$	NA	1 sun (AM1.5) on reduced $SrTiO_3$ and $\lambda > 400$ nm on InP-Ru complex, no external bias, 0.1 M $NaHCO_3$-phosphoric acid (pH=7.7)	FE(HCOOH) = 71.6%, TON> 18 Wired 1.45 μmol (3 h), STC 0.14%; FE(H_2)= 10%, FE(CO)= 15% Wireless: 0.94 μmol HCOOH (3 h), STC 0.08%	NA	[81]
Monolithic Artificial leaves	carbon cloth/p-RuCP	IrO_x	SiGe-jn	1 sun (AM1.5), 0.25 cm^2, 1 sun, AM1.5, no external bias, CO_2-saturated phosphate buffer solution (pH 6.4)	HCOOH: FE= 93% STC 4.6%; H_2 FE= 7%	NA	[82]
Monolithic Artificial leaves	Co(II)O(OH)	WSe_2/ ionic liquid	a-Si-3jn	Cathode side: ionic liquid electrolyte (50%vol:50%vol EMIM-BF_4: deionized water); anode side: KPi solution (pH=7.0)	CO and H_2 (molar ratio ~10:1) STC ~4.6% (due to max efficiency of PV only ~6.0%)	PV only stable for 5 h; replacing PV regularly, the performance artificial leaves were stable during cumulative time of 100 h	[83]

(*continued on next page*)

Table 1 (*continued*)

PEC configurations	Photocathode	(Photo) anode	Photovoltaic	Reaction conditions	Performance	Stability	Reference
Monolithic Artificial leaves	Cu-Zn	Ni foam	4-junction Si	AM 1.5 G (1 sun), 0.5 M $KHCO_3$ (cathode)/ bipolar membrane/1 M KOH (anode) configuration	STC= 4.3%, bias-free current density of 5.0 mA cm^{-2}	FE deceased slightly over 3 h for CO (76%) and H_2 (16%) on average	[84]
Monolithic Artificial leaves	Au/Carbon paper	Ir/ Carbon paper	four-junction space PVs (Z4J)	1 sun (AM1.5), cathode: humidified CO_2 stream, anode: 1 M KOH, 25 °	STC_{syngas} 10.5% (H_2 3.5%, CO 7%), scale-up from 1 to 4 cm^2	Near-constant current density of 8.8 mA cm^{-2} in 3 h	[85]
Monolithic Artificial leaves	CoMTPP@CNT	$BiVO_4$	CsFAMA perovskite	1 sun (AM1.5), 0.5 M $KHCO_3$ buffer	CO 96.4 μmol cm^{-2} FE= 63.6%, H_2 79.8 μmol cm^{-2} FE= 52.6%, O2 40.9 μmol cm^{-2} FE= 57.3%, 185 μA cm^{-2} unassisted photocurrent	100 μA cm^{-2} 67 h	[86]
Monolithic Artificial leaves	CoMTPP@CNT	Ti|$BiVO_4$|TiCo	Flexible CsFAMA perovskite	1 sun irradiation, CO_2-saturated aqueous 0.5 M $KHCO_3$ (pH 7.4)	STC_{CO}= 0.053 ± 0.006% and STH= 0.021 ± 0.004% CO:H_2 = 2.34 ± 0.48	100 cm^2 scaled-up artificial leaves stable over 24 h	[87]
Monolithic Artificial leaves	$Cu_{94}Pd_6$	$BiVO_4$	Inverse-structure $FAMA_{0.22}Pb_{1.32}I_{3.2}Br_{0.66}$	1 sun irradiation, CO_2-saturated aqueous 0.5 M $KHCO_3$ (pH 7.2)	20 h 280 ± 30 μA cm^{-2}, O_2 FE= 7.5% for C_2 +C_3 alcohols 26.9 ± 4.3 μmol cm^{-2}, ethanol 0.58 ± 0.08 μmol cm^{-2}, and n-propanol 0.40 ± 0.03 μmol cm^{-2}, total STC 0.31%	Photocurrent gradually decrease over 20 h	[88]
Monolithic Artificial leaves (semi-artificial)	ClFDH–TiO_2|$CuFeO_2$/CuO	$BiVO_4$/ FeOOH	NA	Xenon lamp (100 mW cm^{-2}, λ > 420 nm), CO_2-saturated phosphate buffer (pH6.5, 50 mM bicarbonate; CO_2 purged for 1 h)	HCOOH 0.098μmol h^{-1} cm^{-2}, FE= 33.5%, STC= 0.008%, external applied bias photon-to-current efficiency 0.20%	Stable photocurrent over 12 h	[93]
Monolithic Artificial leaves (semi-artificial)	FDH|inverse opal TiO_2	$BiVO_4$/ $TiCoO_x$	$Cs_{0.07}FAMA_{0.22}Pb_{1.32}I_{3.27}Br_{0.66}$ perovskite	1 sun (AM 1.5 G), CO_2 atmosphere, stirred, 25 °C in solution of 3-(N-morpholino)-propane sulfonic acid, $NaHCO_3$ and CsCl	HCOOH STC= 0.8%, FE= 83 ± 5%, TON= 1.4 × 10^5, turnover frequency 4 s^{-1}, unbiased current density 0.8 mA cm^{-2}	Photocurrent gradually decrease over 10 h	[94]

causes of performance decline can guide the development of targeted mitigation strategies.

7. Unbiased system considerations: Recognize and address specific challenges related to systems without external bias. Tailoring mitigation approaches to the unique characteristics of unbiased PEC systems can lead to more effective and sustainable solutions.

In brief, the stability of PEC systems is a critical aspect that requires thorough attention. By exploring and implementing the aforementioned strategies, it is possible to mitigate the gradual decrease in performance observed in the majority of the literature, thereby advancing the reliability and long-term functionality of PEC technology.

4. Summary and outlook

The continuous efforts in the field of PEC technologies have yielded exciting advancements. Nevertheless, it is essential to revisit this field and compare it with other technologies. Typically, the realistic photocurrent of photocathodes for CO_2RR is lower than 20 mA cm^{-2} [108]. Consequently, PEC efficiency is still far from reaching the expected theoretical values, and there is currently no well-established and commercially available photocathode. Overall, the efficiencies of PEC technologies, including tandem configurations, remain relatively low, typically falling below 10% [85]. Furthermore, achieving scalability in high-efficiency configurations remains a significant challenge, much like the non-linear relationship between photocatalyst mass and activity. As photoelectrodes are scaled up, they tend to exhibit decreased activity and efficiency compared to their smaller counterparts, with larger scales suffering from various factors such as Ohmic losses, potential drops, and mass transfer limitations [109,110]. In contrast, combining PEC with PV, particularly multiple-junction silicon, emerges as a hybrid technology with higher STC efficiency. The rapid advancements in PV cells continuously push the upper limits of solar-to-electricity efficiency, laying a solid foundation for the enhancement of PV-PEC and artificial leaves, both of which integrate PEC and PV components [25].

PEC technologies directly convert sunlight into chemical energy through solar-driven catalytic reactions utilizing photoactive catalysts. Meanwhile, PV-EC technologies, which exclusively utilize solar energy as their energy source, employ PV as solar-to-electricity converters, and utilize electrolysers for CO_2 reduction, are widely regarded as more promising for commercialization in a near future. The theoretical maximum photocurrents of photoelectrodes generally remain below 20 mA cm^{-2}, with practical values typically much lower. This falls short when compared to electrocatalysis, where currents are often higher by one or two orders of magnitude. While photoelectrodes can directly utilize solar energy to generate photovoltage for driving reactions within a single device, in contrast to the dual-device setup of photovoltaics and

electrolysers and more electron transfer steps [64], PV-EC systems tend to operate much more efficiently than PEC devices. PV-EC can leverage the efficiency of PV cells and subsequent electrochemical processes. Furthermore, the matured state of both electrolysers and silicon PV cells makes commercialization highly feasible in the near future. Despite PV-EC having a briefer history than PEC, the technical maturity of PV cells and electrolysers streamlines system design and capitalizes on existing knowledge and supply chains. This stands in contrast to less mature PEC technologies, which lack commercially available large-scale photoelectrodes or reaction setups. A notable example is the work demonstrating a large-sized PV-EC device (with an irradiation area of approximately 1000 cm^2) for CO_2 reduction to formate [111]. It achieved a STC efficiency of 7.2% with a low operating voltage of 1.85 V (thermodynamic potential 1.43 V), high reaction current of 6.30 A and high formate production rate of 93.5 mmol/h. This system is noteworthy for its high efficiency and cost-effectiveness, as it eliminates usage of membrane (~44% expense of electrolyser). It suggests a bright outlook for PV-EC technology to assume a central role as the primary method for CO_2 reduction. From an economic perspective, the promise of PV-EC is clearly demonstrated in various techno-economic analyses [112]. Recent research has revealed a levelized cost of hydrogen ranging from US$6.22 to 6.70 per kilogram for traditional PV-EC [113,114] and US $9.16 per kilogram for integrated PV-EC [114]. These costs outperform those of PEC systems, which were reported at US$8.43 per kilogram [113] or US$14.60 per kilogram [114]. A study in 2023 reported that the levelized cost of carbon monoxide from PV-EC CO_2RR is US$10.94 per kilogram, with no corresponding data available for PEC [115]. This robust economic potential aligns with the market maturity of PV cells and electrolysers, which exhibit prolonged lifespans of up to a decade, enhancing system durability and reducing maintenance expenses for both components. Furthermore, although capital costs may vary across different PV types, PV-EC is strategically positioned to benefit from economies of scale. Conversely, the future commercialization of PEC technologies remains uncertain, primarily due to the limited practical cost data available for evaluation, especially in the context of CO_2 reduction. However, it should be realized that the high-efficient PV-EC systems come with substantial land use requirements and lack the adaptability that artificial leaves possess to address a wide range of intricate scenarios.

Furthermore, CO_2RR is more intricate than water splitting, requiring a higher thermodynamic energy for CO_2 activation (−1.9 V vs NHE, pH=7) [116] and involving multiple electrons and protons in the reaction pathway, making selectivity challenging to control [117]. While it is relatively straightforward to produce C_1 products like CO, CH_4, and HCOOH, the production of more valuable products, such as alcohols and C_{2+} products, suffers from poor selectivity [118]. The generation of multiple products from CO_2RR poses technical and economic challenges due to the cost of product separation [119]. For instance, although methanol, ethanol, and other alcohols have high market values, the need to recover these low-concentration alcohols from electrolytes makes the overall process less promising for practical applications. Similar issues apply to high-value-added gas-phase products like ethylene and propylene, as obtaining pure high-value products in a single phase has not yet been achieved. It is essential to solve this challenge for direct conversion of CO_2 to high-value chemicals. Addressing this significant challenge is expected to take considerable time.

In this context, alternative approaches for producing high-value chemicals from CO_2RR should be considered. Since achieving high selectivity in single-stage CO_2 reduction systems is challenging, cascade reactions emerge as a promising solution [120,121]. The conversion of CO to high-value carbon products is easier than that of CO_2 due to the critical role of CO as an intermediate, and different catalysts are better suited for its formation and conversion into other carbon species [26, 122]. Furthermore, the presence of CO_2 may hamper the conversion of CO to other chemicals like ethanol [120], which is a primary reason why obtaining pure products other than CO, CH_4, and HCOOH using a single catalyst in a single-stage system is difficult. Instead, specific catalysts can be applied to convert CO produced from CO_2 reduction into target high-value products with significantly higher activity and selectivity [26]. Rather than struggling to enhance selectivity through single-stage CO_2 reduction, developing cascade systems may offer more meaningful and rewarding solutions. Although the costs and operational complexities of cascade systems require careful evaluation, they are likely to be more feasible for industrial production, given that cascade reactions are common in real-world applications.

In addition, as previously stated, while this review primarily concentrates on the coupling of PEC CO_2 reduction with OER, a prevalent approach in current literature, it is worth noting that approximately 90% of the total energy (cell potential) is consumed by OER when examined through thermodynamic analysis [123]. Specifically, OER requires a substantial overpotential, due to its slow kinetics involving a four-electron-transfer process. This sluggishness acts as a hindrance to the overall performance of the PEC tandem system [124]. What is more, oxygen, being relatively low in value, can contribute to challenges in the separation of gas-phase products. Recent insights have highlighted that coupling CO_2RR with alternative oxidation reactions, such as alcohol oxidation, biomass oxidation, or plastic reforming, can substantially reduce energy demands and expedite the overall reaction process [125–127]. Nonetheless, it is important to note that this field is in its early stages of development. Enhancing photocurrent densities by advancing catalysts with higher turnover frequencies remains a critical objective, while addressing challenges related to product selectivity and mitigating mass transport limitations represents substantial research hurdles [124].

Finally, what we would like to underscore is the anticipation that although current techniques may not individually offer the definitive solution to the CO_2 utilization challenge, the ultimate solutions are likely to emerge from the integration of these various technologies. The realization of practical solar-driven CO_2 reduction requires a multidisciplinary approach, drawing upon knowledge and expertise from various related research fields. Even in cases where certain research directions appear less promising, their knowledge and technologies can potentially be integrated with others to contribute to a comprehensive solution. Furthermore, it is not feasible for a single technology to be universally applicable, even though it can excel in most use cases. In specific situations, less efficient technologies may need to be employed either as the primary choice or as an alternative due to specific situational demands. As an illustration, we anticipate continuous advancements in the evolution of artificial leaves, which will serve to reinforce and enhance the capabilities of PV-EC technology. As per the recent research advancements highlighted in this review, the most energy-efficient artificial leaves are found in monolithic wireless PV-EC configurations rather than PV-PEC or PEC-PEC. (Wireless) artificial leaves, offering enhanced simplicity and flexibility, are more ideal, for centralized or distributed integration in various application scenarios on land or water, compared with the wired PV-EC devices. Despite the benefits they offer, the current efficiencies of PV-EC artificial leaves are still inferior to those of conventional wired PV-EC devices. Therefore, there is a need for improvement to enhance the efficiencies of PV-EC artificial leaves. As a result, we expect that continuous advancements in artificial leaves technology will play a pivotal role in fortifying the overall capabilities of PV-EC technology in the future. This will continue until the efficiency of artificial leaves reaches a sufficiently high level, enabling them to assume the primary role.

CRediT authorship contribution statement

Lu Haijiao: Conceptualization, Formal analysis, Investigation, Methodology, Writing – original draft, Writing – review & editing. **Wang Lianzhou:** Conceptualization, Formal analysis, Funding acquisition, Project administration, Writing – review & editing.

Declaration of Competing Interest

The authors declare the following financial interests/personal relationships which may be considered as potential competing interests: Lianzhou Wang reports financial support was provided by Australian Research Council. Haijiao Lu reports financial support was provided by Australian Research Council.

Data Availability

No data was used for the research described in the article.

Acknowledgements

The authors gratefully acknowledge the support from the Australian Research Council through its DECRA (DE230100357), Discovery Project (DP230100621), and Laureate Fellowship (FL190100139) schemes, The University of Queensland through its Research Donation Generic Scheme, and the QUEX institute through its Research Accelerator Grant.

References

[1] D.W. Keith, Why capture CO_2 from the atmosphere? Science 325 (2009) 1654–1655.
[2] T.J. Battin, S. Luyssaert, L.A. Kaplan, A.K. Aufdenkampe, A. Richter, L.J. Tranvik, The boundless carbon cycle, Nat. Geosci. 2 (2009) 598–600.
[3] T.A. Jacobson, J.S. Kler, M.T. Hernke, R.K. Braun, K.C. Meyer, W.E. Funk, Direct human health risks of increased atmospheric carbon dioxide, Nat. Sustain 2 (2019) 691–701.
[4] H.W. Lin, S.N. Luo, H.B. Zhang, J.H. Ye, Toward solar-driven carbon recycling, Joule 6 (2022) 294–314.
[5] J. He, C. Janaky, Recent advances in solar-driven carbon dioxide conversion: expectations versus reality, ACS Energy Lett. 5 (2020) 1996–2014.
[6] J. Albero, Y. Peng, H. Garcia, Photocatalytic CO_2 reduction to C_{2+} products, ACS Catal. 10 (2020) 5734–5749.
[7] S. Jin, What else can photoelectrochemical solar energy conversion do besides water splitting and CO_2 reduction? ACS Energy Lett. 3 (2018) 2610–2612.
[8] B. Tang, F.X. Xiao, An overview of solar-driven photo electrochemical co2 conversion to chemical fuels, ACS Catal. 12 (2022) 9023–9057.
[9] S. Kar, M. Rahaman, V. Andrei, S. Bhattacharjee, S. Roy, E. Reisner, Integrated capture and solar-driven utilization of CO_2 from flue gas and air, Joule 7 (2023) 1496–1514.
[10] J.H. Montoya, L.C. Seitz, P. Chakthranont, A. Vojvodic, T.F. Jaramillo, J. K. Norskov, Materials for solar fuels and chemicals, Nat. Mater. 16 (2017) 70–81.
[11] T. Morikawa, S. Sato, K. Sekizawa, T.M. Suzuki, T. Arai, Solar driven CO_2 reduction using a semiconductor/molecule hybrid photosystem: from photocatalysts to a monolithic artificial leaf, Acc. Chem. Res 55 (2022) 933–943.
[12] M.M. May, K. Rehfeld, Negative emissions as the new frontier of photoelectrochemical CO_2 reduction, Adv. Energy Mater. 12 (2022) 2103801.
[13] K. Sivula, R. van de Krol, Semiconducting materials for photoelectrochemical energy conversion, Nat. Rev. Mater. 1 (2016) 15010.
[14] S.Z. Xu, E.A. Carter, Theoretical insights into heterogeneous (photo) electrochemical CO_2 reduction, Chem. Rev. 119 (2019) 6631–6669.
[15] D. Li, K.X. Yang, J.H. Lian, J.Q. Yan, S.Z. Liu, Powering the world with solar fuels from photoelectrochemical CO_2 reduction: basic principles and recent advances, Adv. Energy Mater. 12 (2022) 2201070.
[16] H.J. Lu, J. Tournet, K. Dastafkan, Y. Liu, Y.H. Ng, S.K. Karuturi, C. Zhao, Z.Y. Yin, Noble-metal-free multicomponent nanointegration for sustainable energy conversion, Chem. Rev. 121 (2021) 10271–10366.
[17] L.K. Putri, B.J. Ng, W.J. Ong, S.P. Chai, A.R. Mohamed, Toward excellence in photocathode engineering for photoelectrochemical CO_2 reduction: design rationales and current progress, Adv. Energy Mater. 12 (2022) 2201093.
[18] S.Y. Chen, L.W. Wang, Thermodynamic oxidation and reduction potentials of photocatalytic semiconductors in aqueous solution, Chem. Mater. 24 (2012) 3659–3666.
[19] H.J. Lu, Z.L. Wang, L.Z. Wang, Photocatalytic and photoelectrochemical carbon dioxide reductions toward value-added multicarbon products, ACS EST Eng. 2 (2022) 975–988.
[20] J.L. White, M.F. Baruch, J.E. Pander, Y. Hu, I.C. Fortmeyer, J.E. Park, T. Zhang, K. Liao, J. Gu, Y. Yan, T.W. Shaw, E. Abelev, A.B. Bocarsly, Light-driven heterogeneous reduction of carbon dioxide: photocatalysts and photoelectrodes, Chem. Rev. 115 (2015) 12888–12935.
[21] D.D. Zhang, J.Y. Shi, W. Zi, P.P. Wang, S.Z. Liu, Recent advances in photoelectrochemical applications of silicon materials for solar-to-chemicals conversion, Chemsuschem 10 (2017) 4324–4341.
[22] X.X. Chang, T. Wang, P.P. Yang, G. Zhang, J.L. Gong, The development of cocatalysts for photoelectrochemical CO_2 reduction, Adv. Mater. 31 (2019) 1804710.
[23] V. Kumaravel, J. Bartlett, S.C. Pillai, Photoelectrochemical conversion of carbon dioxide (CO_2) into fuels and value-added products, ACS Energy Lett. 5 (2020) 486–519.
[24] S. Zhang, Q. Fan, R. Xia, T.J. Meyer, CO_2 reduction: from homogeneous to heterogeneous electrocatalysis, Acc. Chem. Res 53 (2020) 255–264.
[25] C.E. Creissen, M. Fontecave, Solar-driven electrochemical CO_2 reduction with heterogeneous catalysts, Adv. Energy Mater. 11 (2021) 2002652.
[26] C.J. Kong, E.L. Warren, A.L. Greenaway, R.R. Prabhakar, A.C. Tamboli, J. W. Ager, Design principles of tandem cascade photoelectrochemical devices, Sustain Energy Fuels 5 (2021) 6361–6371.
[27] G.G.Y. Yang, W.H. Gu, H. Fu, Y. Wang, B. Cai, H.R. Xia, J.M. Zhang, N. Liang, C. Xing, G.C. Yang, S.C. Chen, Y.W. Huang, W, Perovskite-solar-cell-powered integrated fuel conversion and energy-storage devices, Adv. Mater. (2023) 2300383.
[28] H. Song, S.Q. Luo, H.M. Huang, B.W. Deng, J.H. Ye, Solar-driven hydrogen production: recent advances, challenges, and future perspectives, ACS Energy Lett. 7 (2022) 1043–1065.
[29] C.C. Li, T. Wang, B. Liu, M.X. Chen, A. Li, G. Zhang, M.Y. Du, H. Wang, S.F. Liu, J. L. Gong, Photoelectrochemical CO_2 reduction to adjustable syngas on grain-boundary-mediated a-Si/TiO_2/Au photocathodes with low onset potentials, Energy Environ. Sci. 12 (2019) 923–928.
[30] T. Hisatomi, J. Kubota, K. Domen, Recent advances in semiconductors for photocatalytic and photoelectrochemical water splitting, Chem. Soc. Rev. 43 (2014) 7520–7535.
[31] Y.X. Xu, A.L. Li, T.T. Yao, C.T. Ma, X.W. Zhang, J.H. Shah, H.X. Han, Strategies for efficient charge separation and transfer in artificial photosynthesis of solar fuels, Chemsuschem 10 (2017) 4277–4305.
[32] I. Ganesh, Electrochemical conversion of carbon dioxide into renewable fuel chemicals - the role of nanomaterials and the commercialization, Renew. Sust. Energy Rev. 59 (2016) 1269–1297.
[33] X.D. Li, S.M. Wang, L. Li, Y.F. Sun, Y. Xie, Progress and perspective for in situ studies of CO_2 reduction, J. Am. Chem. Soc. 142 (2020) 9567–9581.
[34] C.R. Jiang, S.J.A. Moniz, A.Q. Wang, T. Zhang, J.W. Tang, Photoelectrochemical devices for solar water splitting - materials and challenges, Chem. Soc. Rev. 46 (2017) 4645–4660.
[35] S. Chu, P.F. Ou, P. Ghamari, S. Vanka, B.W. Zhou, I. Shih, J. Song, Z.T. Mi, Photoelectrochemical CO_2 Reduction into Syngas with the Metal/Oxide Interface, J. Am. Chem. Soc. 140 (2018) 7869–7877.
[36] Y. Hori, Electrochemical CO_2 reduction on metal electrodes, *Mod. Asp. Electrochem.* (2008) 89–189.
[37] A. Bagger, W. Ju, A.S. Varela, P. Strasser, J. Rossmeisl, Electrochemical CO_2 reduction: a classification problem, Chemphyschem 18 (2017) 3266–3273.
[38] J.X. Hu, N.B. Fan, C. Chen, Y.Q. Wu, Z.H. Wei, B. Xu, Y. Peng, M.R. Shen, R. L. Fan, Facet engineering in Au nanoparticles buried in p-Si photocathodes for enhanced photoelectrochemical CO_2 reduction, Appl. Catal. B-Environ. 327 (2023).
[39] J.G. Hou, H.J. Cheng, O. Takeda, H. Zhu, Three-dimensional bimetal-graphene-semiconductor coaxial nanowire arrays to harness charge flow for the photochemical reduction of carbon dioxide, Angew. Chem. Int Ed. 54 (2015) 8480–8484.
[40] K.P. Kuhl, E.R. Cave, D.N. Abram, T.F. Jaramillo, New insights into the electrochemical reduction of carbon dioxide on metallic copper surfaces, Energy Environ. Sci. 5 (2012) 7050–7059.
[41] K. Jiang, R.B. Sandberg, A.J. Akey, X.Y. Liu, D.C. Bell, J.K. Norskov, K.R. Chan, H. T. Wang, Metal ion cycling of Cu foil for selective C-C coupling in electrochemical CO_2 reduction, Nat. Catal. 1 (2018) 111–119.
[42] C.L. Xiao, J. Zhang, Architectural design for enhanced c2 product selectivity in electrochemical CO_2 reduction using cu-based catalysts: a review, ACS Nano 15 (2021) 7975–8000.
[43] I. Roh, S. Yu, C.K. Lin, S. Louisia, S. Cestellos-Blanco, P.D. Yang, Photoelectrochemical CO_2 reduction toward multicarbon products with silicon nanowire photocathodes interfaced with copper nanoparticles, J. Am. Chem. Soc. 144 (2022) 8002–8006.
[44] Q. Shen, J. Ma, X.F. Huang, N.J. Yang, G.H. Zhao, Enhanced carbon dioxide conversion to formate on a multi-functional synergistic photoelectrocatalytic interface, Appl. Catal. B-Environ. 219 (2017) 45–52.
[45] K. Maeda, Metal-complex/semiconductor hybrid photocatalysts and photoelectrodes for CO_2 reduction driven by visible light, Adv. Mater. 31 (2019) 1808205.
[46] T. Arai, S. Sato, K. Uemura, T. Morikawa, T. Kajino, T. Motohiro, Photoelectrochemical reduction of CO_2 in water under visible-light irradiation by a p-type InP photocathode modified with an electropolymerized ruthenium complex, Chem. Commun. 46 (2010) 6944–6946.
[47] T. Arai, S. Tajima, S. Sato, K. Uemura, T. Morikawa, T. Kajino, Selective CO_2 conversion to formate in water using a CZTS photocathode modified with a ruthenium complex polymer, Chem. Commun. 47 (2011) 12664–12666.
[48] H.N. Tian, Molecular catalyst immobilized photocathodes for water/proton and carbon dioxide reduction, Chemsuschem 8 (2015) 3746–3759.
[49] G. Sahara, R. Abe, M. Higashi, T. Morikawa, K. Maeda, Y. Ueda, O. Ishitani, Photoelectrochemical CO_2 reduction using a Ru(II)-Re(I) multinuclear metal complex on a p-type semiconducting NiO electrode, Chem. Commun. 51 (2015) 10722–10725.
[50] J.B. Liu, H.J. Shi, Q. Shen, C.Y. Guo, G.H. Zhao, Efficiently photoelectrocatalyze CO_2 to methanol using Ru(II)-pyridyl complex covalently bonded on TiO_2 nanotube arrays, Appl. Catal. B-Environ. 210 (2017) 368–378.

[51] B. Shan, S. Vanka, T.T. Li, L. Troian-Gautier, M.K. Brennaman, Z.T. Mi, T. J. Meyer, Binary molecular-semiconductor p-n junctions for photoelectrocatalytic CO_2 reduction, Nat. Energy 4 (2019) 290–299.
[52] P.B. Pati, R.W. Wang, E. Boutin, S. Diring, S. Jobic, N. Barreau, F. Odobel, M. Robert, Photocathode functionalized with a molecular cobalt catalyst for selective carbon dioxide reduction in water, Nat. Commun. 11 (2020) 3499.
[53] J.J. Leung, J. Warnan, K.H. Ly, N. Heidary, D.H. Nam, M.F. Kuehneh, E. Reisner, Solar-driven reduction of aqueous CO_2 with a cobalt bis(terpyridine)-based photocathode, Nat. Catal. 2 (2019) 354–365.
[54] S. Roy, M. Miller, J. Warnan, J.J. Leung, C.D. Sahm, E. Reisner, Electrocatalytic and solar-driven reduction of aqueous CO_2 with molecular cobalt phthalocyanine-metal oxide hybrid materials, ACS Catal. 11 (2021) 1868–1876.
[55] Z.B. Wen, S.X. Xu, Y. Zhu, G.Q. Liu, H. Gao, L.C. Sun, F. Li, Aqueous CO_2 reduction on Si photocathodes functionalized by cobalt molecular catalysts/carbon nanotubes, Angew. Chem. Int Ed. 61 (2022) e202201086.
[56] B. Shang, C.L. Rooney, D.J. Gallagher, B.T. Wang, A. Krayev, H. Shema, O. Leitner, N.J. Harmon, L.Q. Xiao, C. Sheehan, S.R. Bottum, E. Gross, J. F. Cahoon, T.E. Mallouk, H.L. Wang, Aqueous photoelectrochemical CO_2 reduction to CO and methanol over a silicon photocathode functionalized with a cobalt phthalocyanine molecular catalyst, Angew. Chem. Int Ed. 62 (2023) e202215213.
[57] U. Kang, S.K. Choi, D.J. Ham, S.M. Ji, W. Choi, D.S. Han, A. Abdel-Wahabe, H. Park, Photosynthesis of formate from CO_2 and water at 1% energy efficiency via copper iron oxide catalysis, Energy Environ. Sci. 8 (2015) 2638–2643.
[58] G. Sahara, H. Kumagai, K. Maeda, N. Kaeffer, V. Artero, M. Higashi, R. Abe, O. Ishitani, Photoelectrochemical reduction of CO_2 coupled to water oxidation using a photocathode with a Ru(II)-Re(I) complex photocatalyst and a CoO_x/TaON photoanode, J. Am. Chem. Soc. 138 (2016) 14152–14158.
[59] S. Sato, T. Arai, T. Morikawa, K. Uemura, T.M. Suzuki, H. Tanaka, T. Kajino, Selective CO_2 conversion to formate conjugated with H_2O oxidation utilizing semiconductor/complex hybrid photocatalysts, J. Am. Chem. Soc. 133 (2011) 15240–15243.
[60] H. Kumagai, G. Sahara, K. Maeda, M. Higashi, R. Abe, O. Ishitani, Hybrid photocathode consisting of a $CuGaO_2$ p-type semiconductor and a Ru(II)-Re(I) supramolecular photocatalyst: non-biased visible-light-driven CO_2 reduction with water oxidation, Chem. Sci. 8 (2017) 4242–4249.
[61] K. Sekizawa, S. Sato, T. Arai, T. Morikawa, Solar-driven photocatalytic CO_2 reduction in water utilizing a ruthenium complex catalyst on p-type Fe_2O_3 with a multiheterojunction, ACS Catal. 8 (2018) 1405–1416.
[62] M.F. Weber, M.J. Dignam, Efficiency of splitting water with semiconducting photoelectrodes, J. Electrochem Soc. 131 (1984) 1258–1265.
[63] J.R. Bolton, S.J. Strickler, J.S. Connolly, Limiting and realizable efficiencies of solar photolysis of water, Nature 316 (1985) 495–500.
[64] M.S. Prevot, K. Sivula, Photoelectrochemical tandem cells for solar water splitting, J. Phys. Chem. C. 117 (2013) 17879–17893.
[65] S. Hu, C.X. Xiang, S. Haussener, A.D. Berger, N.S. Lewis, An analysis of the optimal band gaps of light absorbers in integrated tandem photoelectrochemical water-splitting systems, Energy Environ. Sci. 6 (2013) 2984–2993.
[66] V. Andrei, R.A. Jagt, M. Rahaman, L. Lari, V.K. Lazarov, J.L. MacManus-Driscoll, R.L.Z. Hoye, E. Reisner, Long-term solar water and CO_2 splitting with photoelectrochemical BiOI-$BiVO_4$ tandems, Nat. Mater. 21 (2022) 864–868.
[67] M. Halmann, Photoelectrochemical reduction of aqueous carbon-dioxide on p-type gallium-phosphide in liquid junction solar-cells, Nature 275 (1978) 115–116.
[68] S.C. Wang, G. Liu, L.Z. Wang, Crystal facet engineering of photoelectrodes for photoelectrochemical water splitting, Chem. Rev. 119 (2019) 5192–5247.
[69] J.H. Kim, J.S. Lee, Elaborately modified $BiVO_4$ photoanodes for solar water splitting, Adv. Mater. 31 (2019) 1806938.
[70] R. Tang, S.J. Zhou, Z.Y. Zhang, R.K. Zheng, J. Huang, Engineering nanostructure-interface of photoanode materials toward photoelectrochemical water oxidation, Adv. Mater. 33 (2021) 2005389.
[71] J.B. Pan, S. Shen, L. Chen, C.T. Au, S.F. Yin, Core-shell photoanodes for photoelectrochemical water oxidation, Adv. Funct. Mater. 31 (2021) 2104269.
[72] O. Khaselev, J.A. Turner, A monolithic photovoltaic-photoelectrochemical device for hydrogen production via water splitting, Science 280 (1998) 425–427.
[73] K. Zhang, M. Ma, P. Li, D.H. Wang, J.H. Park, Water splitting progress in tandem devices: moving photolysis beyond electrolysis, Adv. Energy Mater. 6 (2016) 1600602.
[74] Z. Liu, S.E. Sofia, H.S. Laine, M. Woodhouse, S. Wieghold, I.M. Peters, T. Buonassisi, Revisiting thin silicon for photovoltaics: a technoeconomic perspective, Energy Environ. Sci. 13 (2020) 12–23.
[75] K. Yoshikawa, H. Kawasaki, W. Yoshida, T. Irie, K. Konishi, K. Nakano, T. Uto, D. Adachi, M. Kanematsu, H. Uzu, K. Yamamoto, Silicon heterojunction solar cell with interdigitated back contacts for a photoconversion efficiency over 26%, Nat. Energy 2 (2017) 17032.
[76] Interactive Best Research-Cell Efficiency Chart, 2023, pp. https://www.nrel.gov/pv/interactive-cell-efficiency.html.
[77] Y.J. Jang, I. Jeong, J. Lee, J. Lee, M.J. Ko, J.S. Lee, Unbiased sunlight-driven artificial photosynthesis of carbon monoxide from CO_2 using a ZnTe-based photocathode and a perovskite solar cell in tandem, ACS Nano 10 (2016) 6980–6987.
[78] Gurudayal, J.W. Beeman, J. Bullock, H. Wang, J. Eichhorn, C. Towle, A. Javey, F. M. Toma, N. Mathews, J.W. Ager, Si photocathode with Ag-supported dendritic Cu catalyst for CO_2 reduction, Energy Environ. Sci. 12 (2019) 1068–1077.
[79] S.Y. Reece, J.A. Hamel, K. Sung, T.D. Jarvi, A.J. Esswein, J.J.H. Pijpers, D. G. Nocera, Wireless solar water splitting using silicon-based semiconductors and earth-abundant catalysts, Science 334 (2011) 645–648.
[80] K.S. Joya, Y.F. Joya, K. Ocakoglu, R. van de Krol, Water-splitting catalysis and solar fuel devices: artificial leaves on the move, Angew. Chem. Int Ed. 52 (2013) 10426–10437.
[81] T. Arai, S. Sato, T. Kajino, T. Morikawa, Solar CO_2 reduction using H_2O by a semiconductor/metal-complex hybrid photocatalyst: enhanced efficiency and demonstration of a wireless system using $SrTiO_3$ photoanodes, Energy Environ. Sci. 6 (2013) 1274–1282.
[82] T. Arai, S. Sato, T. Morikawa, A monolithic device for CO_2 photoreduction to generate liquid organic substances in a single-compartment reactor, Energy Environ. Sci. 8 (2015) 1998–2002.
[83] M. Asadi, K. Kim, C. Liu, A.V. Addepalli, P. Abbasi, P. Yasaei, P. Phillips, A. Behranginia, J.M. Cerrato, R. Haasch, P. Zapol, B. Kumar, R.F. Klie, J. Abiade, L.A. Curtiss, A. Salehi-Khojin, Nanostructured transition metal dichalcogenide electrocatalysts for CO_2 reduction in ionic liquid, Science 353 (2016) 467–470.
[84] F. Urbain, P.Y. Tang, N.M. Carretero, T. Andreu, L.G. Gerling, C. Voz, J. Arbiol, J. R. Morante, A prototype reactor for highly selective solar-driven CO_2 reduction to synthesis gas using nanosized earth-abundant catalysts and silicon photovoltaics, Energy Environ. Sci. 10 (2017) 2256–2266.
[85] T.A. Kistler, M.Y. Um, J.K. Cooper, I.D. Sharp, P. Agbo, Monolithic photoelectrochemical CO_2 reduction producing syngas at 10% efficiency, Adv. Energy Mater. 11 (2021) 2100070.
[86] V. Andrei, B. Reuillard, E. Reisner, Bias-free solar syngas production by integrating a molecular cobalt catalyst with perovskite-$BiVO_4$ tandems, Nat. Mater. 19 (2020) 189–194.
[87] V. Andrei, G.M. Ucoski, C. Pornrungroj, C. Uswachoke, Q. Wang, D.S. Achilleos, H. Kasap, K.P. Sokol, R.A. Jagt, H.J. Lu, T. Lawson, A. Wagner, S.D. Pike, D. S. Wright, R.L.Z. Hoye, J.L. MacManus-Driscoll, H.J. Joyce, R.H. Friend, E. Reisner, Floating perovskite-$BiVO_4$ devices for scalable solar fuel production, Nature 608 (2022) 518–522.
[88] M. Rahaman, V. Andrei, D. Wright, E. Lam, C. Pornrungroj, S. Bhattacharjee, C. M. Pichler, H.F. Greer, J.J. Baumberg, E. Reisner, Solar-driven liquid multi-carbon fuel production using a standalone perovskite-$BiVO_4$ artificial leaf, Nat. Energy 8 (2023) 629–638.
[89] E.J. Son, J.W. Ko, S.K. Kuk, H. Choe, S. Lee, J.H. Kim, D.H. Nam, G.M. Ryu, Y. H. Kim, C.B. Park, Sunlight-assisted, biocatalytic formate synthesis from CO_2 and water using silicon-based photoelectrochemical cells, Chem. Commun. 52 (2016) 9723–9726.
[90] S.K. Kuk, R.K. Singh, D.H. Nam, R. Singh, J.K. Lee, C.B. Park, Photoelectrochemical reduction of carbon dioxide to methanol through a highly efficient, Enzym. Cascade, Angew. Chem. Int Ed. 56 (2017) 3827–3832.
[91] Y.J. Chen, C.H. Tung, L.Z. Wu, Semi-artificial photoelectrochemical synthesis, Joule 5 (2021) 2771–2773.
[92] B.A. Parkinson, P.F. Weaver, Photoelectrochemical pumping of enzymatic CO_2 reduction, Nature 309 (1984) 148–149.
[93] S.K. Kuk, J. Jang, J. Kim, Y. Lee, Y.S. Kim, B. Koo, Y.W. Lee, J.W. Ko, B. Shin, J. K. Lee, C.B. Park, CO_2-reductive, copper oxide-based photobiocathode for Z-scheme semi-artificial leaf structure, Chemsuschem 13 (2020) 2940–2944.
[94] E.E. Moore, V. Andrei, A.R. Oliveira, A.M. Coito, I.A.C. Pereira, E. Reisner, A. Semi-artificial, Photoelectrochemical tandem leaf with a CO_2-to-formate efficiency approaching 1%, Angew. Chem. Int Ed. 60 (2021) 26303–26307.
[95] Q. Chen, G.Z. Fan, H.W. Fu, Z.S. Li, Z.G. Zou, Tandem photoelectrochemical cells for solar water splitting, Adv. Phys. -X 3 (2018) 1487267.
[96] J. Ronge, T. Bosserez, D. Martel, C. Nervi, L. Boarino, F. Taulelle, G. Decher, S. Bordiga, J.A. Martens, Monolithic cells for solar fuels, Chem. Soc. Rev. 43 (2014) 7963–7981.
[97] N.S. Lewis, Research opportunities to advance solar energy utilization, Science 351 (2016) aad1920.
[98] V. Andrei, Q. Wang, T. Uekert, S. Bhattacharjee, E. Reisner, Solar panel technologies for light-to-chemical conversion, Acc. Chem. Res 55 (2022) 3376–3386.
[99] N.S. Weliwatte, S.D. Minteer, Photo-bioelectrocatalytic CO_2 reduction for a circular energy landscape, Joule 5 (2021) 2564–2592.
[100] S.J. Cobb, V.M. Badiani, A.M. Dharani, A. Wagner, S. Zacarias, A.R. Oliveira, I.A. C. Pereira, E. Reisner, Fast CO_2 hydration kinetics impair heterogeneous but improve enzymatic CO_2 reduction catalysis, Nat. Chem. 14 (2022) 417–424.
[101] H. Homayoni, W. Chanmanee, N.R. de Tacconi, B.H. Dennis, K. Rajeshwar, Continuous flow photoelectrochemical reactor for solar conversion of carbon dioxide to alcohols, J. Electrochem Soc. 162 (2015) E115–E122.
[102] P.Q. Li, J.F. Xu, H. Jing, C.X. Wu, H. Peng, J. Lu, H.Z. Yin, Wedged N-doped CuO with more negative conductive band and lower overpotential for high efficiency photoelectric converting CO_2 to methanol, Appl. Catal. B-Environ. 156 (2014) 134–140.
[103] S.T. Guo, Z.Y. Tang, T. Liu, T. Ouyang, Z.Q. Liu, Chlorine anion stabilized Cu_2O/ZnO photocathode for selective CO_2 reduction to CH_4, Appl. Catal. B-Environ. 321 (2023) 122035.
[104] X. Ba, L.L. Yan, S. Huang, J.G. Yu, X.J. Xia, Y. Yu, New way for CO_2 reduction under visible light by a combination of a Cu electrode and semiconductor thin film: Cu_2O conduction type and morphology effect, J. Phys. Chem. C. 118 (2014) 24467–24478.
[105] K.K. Wang, Y. Liu, Q.M. Wang, Y.F. Zhang, X.T. Yang, L. Chen, M. Liu, X.Q. Qiu, J. Li, W.Z. Li, Asymmetric Cu-N sites on copper oxide photocathode for photoelectrochemical CO_2 reduction towards C_2 products, Appl. Catal. B-Environ. 316 (2022) 121616.

[106] N. Sagara, S. Kamimura, T. Tsubota, T. Ohno, Photoelectrochemical CO_2 reduction by a p-type boron-doped g-C_3N_4 electrode under visible light, Appl. Catal. B-Environ. 192 (2016) 193–198.
[107] N.C.D. Nath, S.Y. Choi, H.W. Jeong, J.J. Lee, H. Park, Stand-alone photoconversion of carbon dioxide on copper oxide wire arrays powered by tungsten trioxide/dye-sensitized solar cell dual absorbers, Nano Energy 25 (2016) 51–59.
[108] J.W. Jang, S. Cho, G. Magesh, Y.J. Jang, J.Y. Kim, W.Y. Kim, J.K. Seo, S. Kim, K. H. Lee, J.S. Lee, Aqueous-solution route to zinc telluride films for application to CO_2 reduction, Angew. Chem. Int Ed. 53 (2014) 5852–5857.
[109] H.J. Lu, V. Andrei, K. Jenkinson, A. Regoutz, N. Li, C.E. Creissen, A.E. H. Wheatley, H.X. Hao, E. Reisner, D.S. Wright, S.D. Pike, Single-source bismuth (transition metal) polyoxovanadate precursors for the scalable synthesis of doped $BiVO_4$ photoanodes, Adv. Mater. 30 (2018) 1804033.
[110] S. Dilger, M. Trottmann, S. Pokrant, Scaling Up electrodes for photoelectrochemical water splitting: fabrication process and performance of 40cm^2 $LaTiO_2N$ photoanodes, Chemsuschem 12 (2019) 1931–1938.
[111] N. Kato, S. Mizuno, M. Shiozawa, N. Nojiri, Y. Kawai, K. Fukumoto, T. Morikawa, Y. Takeda, A large-sized cell for solar-driven CO_2 conversion with a solar-to-formate conversion efficiency of 7.2, Joule 5 (2021) 687–705.
[112] Y. Zhang, C.L. Ye, J.J. Duan, H. Feng, D. Liu, Q. Li, Solar-driven carbon dioxide reduction: a fair evaluation of photovoltaic-biased photoelectrocatalysis and photovoltaic-powered electrocatalysis, Front Energy Res 10 (2022) 956444.
[113] A. Grimm, W.A. de Jong, G.J. Kramer, Renewable hydrogen production: a techno-economic comparison of photoelectrochemical cells and photovoltaic-electrolysis, Int J. Hydrog. Energy 45 (2020) 22545–22555.
[114] Z.X. Li, S. Fang, H.D. Sun, R.J. Chung, X.S. Fang, J.H. He, Solar hydrogen, Adv. Energy Mater. 13 (2023) 2203019.
[115] S.Y. Chae, S.Y. Lee, S.G. Han, H. Kim, J. Ko, S. Park, O.S. Joo, D. Kim, Y. Kang, U. Lee, Y.J. Hwang, B.K. Min, A perspective on practical solar to carbon monoxide production devices with economic evaluation, Sustain Energy Fuels 4 (2020) 199–212.
[116] W.H. Koppenol, J.D. Rush, Reduction potential of the carbon dioxide/carbon dioxide radical anion: a comparison with other C_1 radicals, J. Phys. Chem. 91 (1987) 4429–4430.
[117] J.H. Wu, Y. Huang, W. Ye, Y.G. Li, CO_2 reduction: from the electrochemical to photochemical approach, Adv. Sci. 4 (2017) 1700194.
[118] S. Nitopi, E. Bertheussen, S.B. Scott, X.Y. Liu, A.K. Engstfeld, S. Horch, B. Seger, I. E.L. Stephens, K. Chan, C. Hahn, J.K. Norskov, T.F. Jaramillo, I. Chorkendorff, Progress and perspectives of electrochemical CO_2 reduction on copper in aqueous electrolyte, Chem. Rev. 119 (2019) 7610–7672.
[119] G.H. Lee, A.S. Rasouli, B.H. Lee, J.Q. Zhang, D.H. Won, Y.C. Xiao, J.P. Edwards, M.G. Lee, E.D. Jung, F. Arabyarmohammadi, H.Z. Liu, I. Grigioni, J. Abed, T. Alkayyali, S.J. Liu, K. Xie, R.K. Miao, S. Park, R. Dorakhan, Y. Zhao, C. P. O'Brien, Z. Chen, D. Sinton, E. Sargent, CO_2 electroreduction to multicarbon products from carbonate capture liquid, Joule 7 (2023) 1277–1288.
[120] N. Theaker, J.M. Strain, B. Kumar, J.P. Brian, S. Kumari, J.M. Spurgeon, Heterogeneously catalyzed two-step cascade electrochemical reduction of CO_2 to ethanol, Electro Acta 274 (2018) 1–8.
[121] B.A. Zhang, D.G. Nocera, Cascade electrochemical reduction of carbon dioxide with bimetallic nanowire and foam electrodes, Chemelectrochem 8 (2021) 1918–1924.
[122] M. Zheng, P.T. Wang, X. Zhi, K. Yang, Y. Jiao, J.J. Duan, Y. Zheng, S.Z. Qiao, Electrocatalytic CO_2-to-C_{2+} with ampere-level current on heteroatom-engineered copper via tuning *CO intermediate, J. Am. Chem. Soc. 144 (2022) 14936–14944.
[123] S. Verma, S. Lu, P.J.A. Kenis, Co-electrolysis of CO_2 and glycerol as a pathway to carbon chemicals with improved technoeconomics due to low electricity consumption, Nat. Energy 4 (2019) 466–474.
[124] C.R. Lhermitte, K. Sivula, Alternative oxidation reactions for solar-driven fuel production, ACS Catal. 9 (2019) 2007–2017.
[125] D.E.M. Antón-García, E. Bajada, M.A. Eisenschmidt, A. Oliveira, A.R. Pereira, I.A. C. Warnan, J. Reisner, E, Photoelectrochemical hybrid cell for unbiased CO_2 reduction coupled to alcohol oxidation, Nat. Synth. 1 (2022) 77–86.
[126] S.R. Bhattacharjee, Motiar Andrei, Virgil Miller, Melanie Rodríguez-Jiménez, Santiago Lam, Erwin Pornrungroj, Chanon Reisner, Erwin, Photoelectrochemical CO_2-to-fuel conversion with simultaneous plastic reforming, Nat. Synth. 2 (2023) 182–192.
[127] Y.Y. Pan, H.Y. Zhang, B.W. Zhang, F. Gong, J.Y. Feng, H.T. Huang, S. Vanka, R. L. Fan, Q. Cao, M.R. Shen, Z.S. Li, Z.A. Zou, R. Xiao, S. Chu, Renewable formate from sunlight, biomass and carbon dioxide in a photoelectrochemical cell, Nat. Commun. 14 (2023) 1013.